



UPPSALA
UNIVERSITET

ViEWS
PREDICTING CONFLICT



Constituent models, *pgm*.

Online appendix C to ViEWS₂₀₂₀: Revising and evaluating the ViEWS
political Violence Early-Warning System.

Håvard Hegre^{1,2}, Curtis Bell^{1,3}, Michael Colaresi^{1,4}, Mihai Croicu¹, Frederick Hoyles¹, Remco
Jansen¹, Maxine Ria Leis¹, Angelica Lindqvist-McGowan¹, David Randahl¹, Espen
Geelmuyden Rød¹, and Paola Vesco¹

¹Department of Peace and Conflict Research, Uppsala University

²Peace Research Institute Oslo

³U.S. Naval War College

⁴University of Pittsburgh

January 21, 2021

Abstract

This appendix documents all the constituent models in the ensembles at the PRIO-GRID-month (*pgm*) level. We give an overview of the main estimation/machine-learning techniques. We describe and motivate each model, report the importance of the main features, and show prediction maps for selected steps for the 2020–2022 period.

CONTENTS

| | |
|--|----------|
| C-1 Estimation of constituent models | 4 |
| C-2 Handling forecasting dynamics | 4 |
| Dynamic simulation | 4 |
| ‘One-step-ahead’ modeling | 5 |
| C-3 Overview of <i>pgm</i> models | 5 |
| C-3.1 History (hist_legacy) | 6 |
| Description | 6 |
| Estimation details | 6 |
| Feature importances | 6 |
| Change history | 7 |
| C-3.2 Spacetime (sptime) | 7 |
| Description | 7 |
| Estimation details | 8 |
| Feature importances | 8 |
| Change history | 9 |
| C-3.3 Onset (onset24_1_all, onset24_100_all) | 10 |
| Description | 10 |
| Estimation details | 10 |
| Change history | 10 |
| Feature importances | 10 |
| C-3.4 Natural geography (pgd_natural) | 14 |
| Description | 14 |
| Estimation details | 14 |
| Feature importances | 14 |
| Change history | 15 |
| C-3.5 Social geography (pgd_social) | 15 |
| Description | 15 |
| Estimation details | 15 |
| Feature importances | 15 |
| Change history | 16 |
| C-3.6 SPEI (spei_full) | 16 |
| Description | 16 |
| Estimation details | 16 |
| Change history | 16 |
| Feature importances | 16 |
| C-3.7 Dynasim (ds_dummy, ds_25) | 18 |
| Description | 18 |
| Estimation details | 18 |
| Change history | 18 |
| C-3.8 All Themes (all_themes) | 18 |
| Description | 18 |
| Estimation details | 18 |
| Change history | 19 |
| Feature importances | 19 |

| | |
|--|-----------|
| C-3.9 Cross Level (crosslevel) | 20 |
| Description | 20 |
| Estimation details | 21 |
| Change history | 21 |
| C-3.10 XGBoost All (xgb_all) | 21 |
| Description | 21 |
| Estimation details | 21 |
| Change history | 23 |
| C-4 Changes in <i>pgm</i> models | 23 |
| C-5 Detailed descriptions, constituent models | 24 |
| C-5.1 State-based conflict (sb) | 24 |
| Prediction maps, forecasts (sb) | 24 |
| C-5.2 One-sided violence (os) | 28 |
| Prediction maps, forecasts (os) | 28 |
| C-5.3 Non-state conflict (ns) | 30 |
| Prediction maps, forecasts (ns) | 30 |
| References | 33 |

C-1 ESTIMATION OF CONSTITUENT MODELS

ViEWS relies on logistic regression, random forest (RF) and gradient boosting machines (GBM) models. The logit model is a generalized linear model (GLM) that performs well compared to many machine-learning techniques (Géron, 2017). Computational costs are low, and with large datasets like ours overfitting is not a serious concern. Both RF models (Breiman, 2001; Muchlinski et al., 2016) and GBM models (Friedman, 2001; Chen and Guestrin, 2016) are machine-learning techniques employing classification and regression trees (CART). In CART, the response variable Y is predicted using a decision tree and some predictor variables X . The tree consists of a number of ‘splits’ into different branches. Each split is found by searching all values in X to find the constant which maximally separates between the categories of Y . The tree continues to be split until some threshold is achieved (to avoid overfitting).

In RF models, CART trees are combined with bootstrap-aggregating (bagging), and random feature selection. Bagging creates an ensemble of trees, each slightly different. These trees are, however, correlated as some variables are especially good at discriminating Y . To avoid this, a random subset of variables (predictors or features) are selected for each ‘split’, solving the correlation problem and creating a forest of uncorrelated ‘random’ trees.

In GBM models, an ensemble of CART trees are trained in an additive, iterative fashion. At each iteration, a new CART tree (a new learner) is added to the ensemble, grown in such a way as to minimize a chosen, derivable, loss function capturing remaining classification or regression error. In practice, this is done by training each new tree on a regularized form of the residuals computed between the ensemble predictions at the previous step and the observed values. Each such new tree is added to the ensemble, and the iterative process is restarted (Friedman, 2001; Chen and Guestrin, 2016). This iterative improvement is referred to as ‘boosting’; this iterative minimization of residual-based loss functions is equivalent with gradient descent. ViEWS uses the XGBoost implementation of GBM, an implementation that adds a regularized learning objective adding a complexity penalty to tree growing and smoothing final learned weights, as well as implementing the same random feature selection and sub-sampling of data (Chen and Guestrin, 2016).

RF and XGB models are memory-intensive to estimate given the computational capacity available for ViEWS. Hence, at the *pgm* level, we estimate them using a ‘downsampled’ dataset which includes all conflict events and a random sample of non-events (see details in the ‘Overview of models’ section in this appendix).

C-2 HANDLING FORECASTING DYNAMICS

ViEWS employs two alternative strategies to compute forecasts for each of $s \in (1, \dots, 36)$ months into the future. We call these Dynamic simulation (*ds*) and One-step-ahead (*osa*).

Dynamic simulation

The dynamic simulation (Dynamism) procedure builds on Hegre et al. (2013) and Hegre et al. (2016), and is discussed at length there.¹ The procedure involves simulating model parameters based on the estimated coefficients and the variance-covariance matrix from a model. In addition, we compute predicted probabilities for the outcomes for the first month t , draw outcomes, recalculate the history variables so that the input predictor matrix X_{t+1} at $t+1$ reflects that draw. This is repeated for each month s in the forecasting window, and for each simulated set of parameters.

If we are interested in forecasting two months into the forecasting period, we first train the constituent models, estimate the weights, and produce our ensemble one-month-ahead forecast. To produce forecasts

¹The first author’s original script ‘PRIOsim’ was rewritten in C# and C++ by Joakim Karlsen. The Python routines underlying the current projects are based on the ‘Dynamism’ reimplementations of this, written by Jonas Vestby and Frederick Hoyles.

for the next month, we need the input predictor matrices $X_{t+1}^{(k)}$. For many constituent models, these input predictors will themselves be functions of actual conflict (e.g., lagged conflict indicators, time since last conflict, spatial distance to nearest conflict). Since these do not exist for the next month (after the training window), we use the prediction as the probability of an unobserved predictor, for example for conflict at time $t + 1$, when forecasting conflict at $t + 2$. A simulated value is drawn from this probability, and recorded within a new simulated set of predictors $\tilde{X}_{t+1}^{(k)}$.

The predictions for the three outcomes are obtained simultaneously within each time step. For each of these, we compute the predicted probability at $t + 1$ as a function of information available at t , including the status for the other two outcomes. This procedure repeats for every month to the end of the forecasting window.

'One-step-ahead' modeling

In the 'one-step-ahead' modeling, we predict each step into the future ($t + 1$, (...), $t + 12$, (...) $t + 36$) independently, as opposed to dynamic simulation which moves forward sequentially. We do this by estimating a set of models of the form $f_s(X_{t-s})$ where s denotes the number of months into the future to forecast. In regression notation these take the form $y_{t+s} = X_t\beta_t$, for $s \in (1, 36)$. The 'one-step-ahead' model does this by time-shifting the right-hand side variables with respect to the outcome before models are trained, making the model a link function between the future (y_{t+s}) and the present (X_t).

C-3 OVERVIEW OF PGM MODELS

Pgm models are built according to themes which can be combined in increasing levels of complexity. The basic themes include History, Sptime, Institutional, Oil, Natural Geography, Social Geography and SPEI (drought).

Model name

| |
|-----------------|
| hist_legacy |
| sptime |
| onset24_100_all |
| onset24_1_all |
| pgd_natural |
| pgd_social |
| spei_full |
| ds_25 |
| ds_dummy |
| allthemes |
| crosslevel |
| xgb |

Table C-1. Models in the *cm* ensemble as of r.2020.02.01

We have defined a set of 'models' characterized by a set of features as well as an estimation procedure. All models are trained for each of the three different types of conflict, i.e. state-based (**sb**), non-state (**ns**) and one-sided (**os**) violence, as well as for all steps s .

If nothing else is stated, the estimator is the random forest classifier (Breiman, 2001) from the scikit-learn package (Pedregosa et al., 2011). All parameters used are the package defaults, except for $n_estimators$ which controls the number of trees in the forest and is set to 1000.

With these settings the procedure works as follows: for each of 1000 trees, draw a bootstrapped sample of the same size as the training data. On this sample, fit a decision tree using the gini split quality criterion, considering the square root of the number of features for each split. Predicted probabilities from the forest are computed as the average of the predicted probability from each tree, which is the fraction of samples for the class in the current leaf of the tree.

Feature importances are a measure of the importance of each feature in the forest. Below, we present impurity-based features importances.² The importances of all features sum to one and are assigned according to the position of the feature in the trained trees, with features appearing higher up in the trees receiving a higher score as the expected fraction of samples they contribute to predicting is higher.

Below, we present a description of the model features used as predictors for the different dependent variables. The following sections will provide further details on the types of outcome which is predicted.

C-3.1 History (*hist_legacy*)

Description

The history model traces the conflict history of a grid-cell, based on the evidence showing a higher conflict incidence in locations which experienced conflict in the past (Collier, Hegre, and Raknerud, 2003). The model includes 1-12 temporal lags of the specific dependent variable, such as incidence of state-based violence. Moreover, the specific outcome is temporally lagged by 1-3 months for the cells adjacent to the conflictual grid cell. Also included are the other dependent variables lagged by 1 month, both for each grid cell and all the neighboring cells. Finally, the model includes a 12-months half-life decay function of the time since a conflict event occurred for all dependent variables.

Estimation details

The model uses the 'one-step-ahead' approach (see Section C-2) and is estimated on data for Africa only.

Feature importances

The tables below report the feature importances for each type of violence and different time steps ($s = 1, 3, 6, 12, 24, 36$). Please note that for broad models like *hist_legacy*, the tables report only the first 25 most important features. The 12-months decay function of the last conflict episode is the most important feature to predict violence of any type. The most important feature is not strictly outcome-specific; time since last **sb** conflict is the most relevant variable to predict both **sb** and **os**, while time since last **os** and **ns** violence are the most relevant variable to predict **ns** conflict.

²For a critical review of impurity-based feature importances, see Strobl et al. (2007) and Strobl et al. (2008)

| sb_hist_legacy | 1 | 3 | 6 | 12 | 24 | 36 |
|------------------------------------|----------|----------|----------|----------|----------|----------|
| decay_12_time_since_ged_dummy_sb | 0.121231 | 0.119443 | 0.117021 | 0.124543 | 0.127912 | 0.134342 |
| decay_12_time_since_ged_dummy_os | 0.112707 | 0.117378 | 0.121663 | 0.128593 | 0.137806 | 0.151205 |
| decay_12_time_since_ged_dummy_ns | 0.068922 | 0.072056 | 0.075678 | 0.081365 | 0.091652 | 0.102848 |
| tlag_1_ged_dummy_sb | 0.067318 | 0.065875 | 0.062689 | 0.054182 | 0.041584 | 0.039771 |
| decay_12_time_since_acled_dummy_pr | 0.061117 | 0.063602 | 0.065700 | 0.069556 | 0.074375 | 0.081557 |
| tlag_3_ged_dummy_sb | 0.051518 | 0.039368 | 0.048652 | 0.045230 | 0.040391 | 0.026612 |
| tlag_2_ged_dummy_sb | 0.050512 | 0.055556 | 0.046442 | 0.044761 | 0.047562 | 0.038962 |
| tlag_4_ged_dummy_sb | 0.043669 | 0.043064 | 0.040543 | 0.033727 | 0.034569 | 0.030552 |
| tlag_3_splag_1_1_ged_dummy_sb | 0.037127 | 0.036443 | 0.036217 | 0.036648 | 0.037098 | 0.039536 |
| tlag_1_splag_1_1_ged_dummy_sb | 0.036771 | 0.036650 | 0.035561 | 0.036323 | 0.037681 | 0.038045 |
| tlag_2_splag_1_1_ged_dummy_sb | 0.036729 | 0.036236 | 0.036115 | 0.035924 | 0.037551 | 0.038349 |
| tlag_9_ged_dummy_sb | 0.036539 | 0.029030 | 0.034238 | 0.035560 | 0.030200 | 0.026418 |
| tlag_8_ged_dummy_sb | 0.036501 | 0.034741 | 0.029745 | 0.027167 | 0.029051 | 0.029455 |
| tlag_7_ged_dummy_sb | 0.034952 | 0.036619 | 0.034124 | 0.036397 | 0.026527 | 0.029480 |
| tlag_5_ged_dummy_sb | 0.034915 | 0.037552 | 0.039093 | 0.034391 | 0.033162 | 0.031315 |
| tlag_6_ged_dummy_sb | 0.034385 | 0.035929 | 0.035640 | 0.030899 | 0.029772 | 0.028529 |
| tlag_10_ged_dummy_sb | 0.029613 | 0.027659 | 0.027620 | 0.034612 | 0.026498 | 0.022936 |
| tlag_1_splag_1_1_ged_dummy_os | 0.026441 | 0.026612 | 0.026404 | 0.026331 | 0.028392 | 0.029392 |
| tlag_11_ged_dummy_sb | 0.026185 | 0.026413 | 0.029094 | 0.024950 | 0.027053 | 0.021653 |
| tlag_12_ged_dummy_sb | 0.022991 | 0.028948 | 0.027576 | 0.028740 | 0.029322 | 0.026476 |
| tlag_1_splag_1_1_acled_dummy_pr | 0.015094 | 0.015875 | 0.015183 | 0.015667 | 0.016526 | 0.017133 |
| tlag_1_splag_1_1_ged_dummy_ns | 0.006802 | 0.007045 | 0.007094 | 0.006503 | 0.007159 | 0.007094 |
| tlag_1_ged_dummy_os | 0.006197 | 0.006164 | 0.006226 | 0.006192 | 0.006434 | 0.006518 |
| tlag_1_ged_dummy_ns | 0.001765 | 0.001741 | 0.001684 | 0.001740 | 0.001723 | 0.001823 |

Table C-2. Feature importances for the history model, **sb**

| os_hist_legacy | 1 | 3 | 6 | 12 | 24 | 36 |
|------------------------------------|----------|----------|----------|----------|----------|----------|
| decay_12_time_since_ged_dummy_sb | 0.147846 | 0.155234 | 0.162215 | 0.172716 | 0.185132 | 0.196111 |
| decay_12_time_since_ged_dummy_os | 0.123162 | 0.126667 | 0.129812 | 0.136369 | 0.146676 | 0.156496 |
| decay_12_time_since_ged_dummy_ns | 0.120364 | 0.126126 | 0.133293 | 0.142658 | 0.151221 | 0.162635 |
| decay_12_time_since_acled_dummy_pr | 0.092971 | 0.096245 | 0.098423 | 0.100444 | 0.104508 | 0.109688 |
| tlag_1_splag_1_1_ged_dummy_sb | 0.048805 | 0.047756 | 0.047556 | 0.045033 | 0.044509 | 0.040315 |
| tlag_1_splag_1_1_ged_dummy_os | 0.048682 | 0.046253 | 0.043965 | 0.042208 | 0.041186 | 0.038556 |
| tlag_3_splag_1_1_ged_dummy_os | 0.046852 | 0.046058 | 0.044464 | 0.042540 | 0.040347 | 0.037783 |
| tlag_2_splag_1_1_ged_dummy_os | 0.046820 | 0.045120 | 0.044127 | 0.043404 | 0.040565 | 0.036952 |
| tlag_1_splag_1_1_acled_dummy_pr | 0.029159 | 0.028074 | 0.027072 | 0.028041 | 0.027987 | 0.026682 |
| tlag_1_ged_dummy_os | 0.028104 | 0.025499 | 0.023043 | 0.017774 | 0.013709 | 0.012631 |
| tlag_2_ged_dummy_os | 0.026436 | 0.024043 | 0.020746 | 0.018228 | 0.015578 | 0.012837 |
| tlag_5_ged_dummy_os | 0.023677 | 0.019453 | 0.019823 | 0.017167 | 0.014255 | 0.013309 |
| tlag_3_ged_dummy_os | 0.023588 | 0.024263 | 0.021586 | 0.018947 | 0.014648 | 0.013357 |
| tlag_4_ged_dummy_os | 0.023281 | 0.021775 | 0.018347 | 0.017288 | 0.015333 | 0.014145 |
| tlag_1_splag_1_1_ged_dummy_ns | 0.021444 | 0.020896 | 0.020785 | 0.019284 | 0.018218 | 0.015913 |
| tlag_6_ged_dummy_os | 0.020947 | 0.019773 | 0.021593 | 0.016769 | 0.014789 | 0.014504 |
| tlag_11_ged_dummy_os | 0.019951 | 0.017989 | 0.017307 | 0.017951 | 0.016400 | 0.013850 |
| tlag_7_ged_dummy_os | 0.019010 | 0.017970 | 0.017357 | 0.016928 | 0.015343 | 0.013167 |
| tlag_8_ged_dummy_os | 0.018790 | 0.018987 | 0.018010 | 0.017048 | 0.016768 | 0.014295 |
| tlag_10_ged_dummy_os | 0.018149 | 0.017651 | 0.017923 | 0.018861 | 0.014983 | 0.013977 |
| tlag_9_ged_dummy_os | 0.017813 | 0.019777 | 0.018331 | 0.016505 | 0.015767 | 0.013995 |
| tlag_12_ged_dummy_os | 0.017578 | 0.018570 | 0.018072 | 0.018173 | 0.016870 | 0.015414 |
| tlag_1_ged_dummy_sb | 0.010938 | 0.010681 | 0.010882 | 0.010409 | 0.010528 | 0.009396 |
| tlag_1_ged_dummy_ns | 0.005633 | 0.005140 | 0.005270 | 0.005257 | 0.004682 | 0.003990 |

Table C-3. Feature importances for the history model, **os**

Change history

The model has been in use since r.2020.02.01

C-3.2 Spacetime (sptime)

Description

The spacetime model includes a set of features that reflect both time and space proximity to conflict and thus comprehensively captures the tendency of conflicts to cluster in space and time (Buhaug and Gleditsch, 2008). A 'spacetime' feature maps the distance to a conflict episode across three dimensions, i.e. longitude,

| ns_hist_legacy | 1 | 3 | 6 | 12 | 24 | 36 |
|------------------------------------|----------|----------|----------|----------|----------|----------|
| decay_12_time_since_ged_dummy_os | 0.146669 | 0.154492 | 0.159657 | 0.167275 | 0.177262 | 0.181365 |
| decay_12_time_since_ged_dummy_ns | 0.126797 | 0.128753 | 0.135104 | 0.142163 | 0.155602 | 0.166558 |
| decay_12_time_since_ged_dummy_sb | 0.115306 | 0.118566 | 0.120641 | 0.120185 | 0.123179 | 0.127904 |
| decay_12_time_since_acled_dummy_pr | 0.104075 | 0.106462 | 0.106806 | 0.107641 | 0.106343 | 0.113010 |
| tlag_1_ged_dummy_ns | 0.040552 | 0.028038 | 0.025057 | 0.023947 | 0.017046 | 0.015778 |
| tlag_1_splag_1_1_ged_dummy_ns | 0.037741 | 0.038204 | 0.034405 | 0.039750 | 0.045939 | 0.048320 |
| tlag_3_splag_1_1_ged_dummy_ns | 0.036659 | 0.033044 | 0.037391 | 0.039577 | 0.044778 | 0.047125 |
| tlag_2_splag_1_1_ged_dummy_ns | 0.034698 | 0.033552 | 0.035295 | 0.044930 | 0.046209 | 0.044969 |
| tlag_1_splag_1_1_acled_dummy_pr | 0.032681 | 0.030610 | 0.029228 | 0.029617 | 0.031671 | 0.028809 |
| tlag_2_ged_dummy_ns | 0.030904 | 0.032474 | 0.025427 | 0.019968 | 0.018908 | 0.018265 |
| tlag_4_ged_dummy_ns | 0.030325 | 0.023098 | 0.028586 | 0.023489 | 0.015699 | 0.016597 |
| tlag_1_splag_1_1_ged_dummy_os | 0.026589 | 0.025999 | 0.025442 | 0.025598 | 0.024778 | 0.026362 |
| tlag_9_ged_dummy_ns | 0.025401 | 0.025758 | 0.017888 | 0.023880 | 0.021565 | 0.014023 |
| tlag_8_ged_dummy_ns | 0.024421 | 0.028771 | 0.021433 | 0.018288 | 0.018579 | 0.015360 |
| tlag_3_ged_dummy_ns | 0.024212 | 0.027350 | 0.026309 | 0.021018 | 0.019326 | 0.015155 |
| tlag_5_ged_dummy_ns | 0.023981 | 0.022973 | 0.026937 | 0.017003 | 0.016282 | 0.013546 |
| tlag_10_ged_dummy_ns | 0.023721 | 0.022652 | 0.027341 | 0.022045 | 0.017884 | 0.015825 |
| tlag_11_ged_dummy_ns | 0.022546 | 0.019509 | 0.018841 | 0.022052 | 0.017724 | 0.015942 |
| tlag_12_ged_dummy_ns | 0.021999 | 0.017345 | 0.020502 | 0.024026 | 0.018679 | 0.018482 |
| tlag_6_ged_dummy_ns | 0.021803 | 0.026471 | 0.025325 | 0.019579 | 0.017503 | 0.015826 |
| tlag_7_ged_dummy_ns | 0.019736 | 0.027091 | 0.024413 | 0.020364 | 0.019195 | 0.014202 |
| tlag_1_splag_1_1_ged_dummy_sb | 0.017531 | 0.017532 | 0.017384 | 0.017482 | 0.016071 | 0.016460 |
| tlag_1_ged_dummy_os | 0.006798 | 0.006557 | 0.006032 | 0.006082 | 0.006009 | 0.006296 |
| tlag_1_ged_dummy_sb | 0.004854 | 0.004697 | 0.004556 | 0.004043 | 0.003769 | 0.003822 |

Table C-4. Feature importances for the history model, **ns**

latitude (the spatial coordinates, measured in spatial degrees) and the time-span. The spacetime feature is therefore a synthetic, multidimensional representation of distance, where each of the three dimensions contribute to the final measure of proximity/distance to conflict. The model includes a number of features with different weightings of time proximity for model space proximity. In one such spacetime feature, a violent event that occurred in cell x at time $t - 1$ is considered to be equally distant in spacetime as a violent event that occurred in the same time-period t in a location which is 1 spatial degree away from the reference point. In each case, the spacetime distance is equal to 1. In other features included in the model, we vary the scale of the time dimension by multiplying the time dimension of this event space by a scalar (we use 0.01, 1 and 10). By shrinking this time scaling factor we can put temporally distant events relatively closer to each grid month, making the space-time tend toward the time since event in the same cell by making spatial distances comparatively large. Conversely, scaling time up makes the feature tend closer to a pure spatial distance where events further back in time are rarely closer than spatially proximate events. The spacetime feature algorithm is essentially a nearest neighbor algorithm and so in principle supports computing the average distance to the k nearest events. We have limited ourselves to the $k = 1$ case of the single nearest neighbor. For maps demonstrating the shifted time scale, see Figure C-1. Included is two variants: space time only (sptime) and one including all themes except history (sptime_and_all_themes).

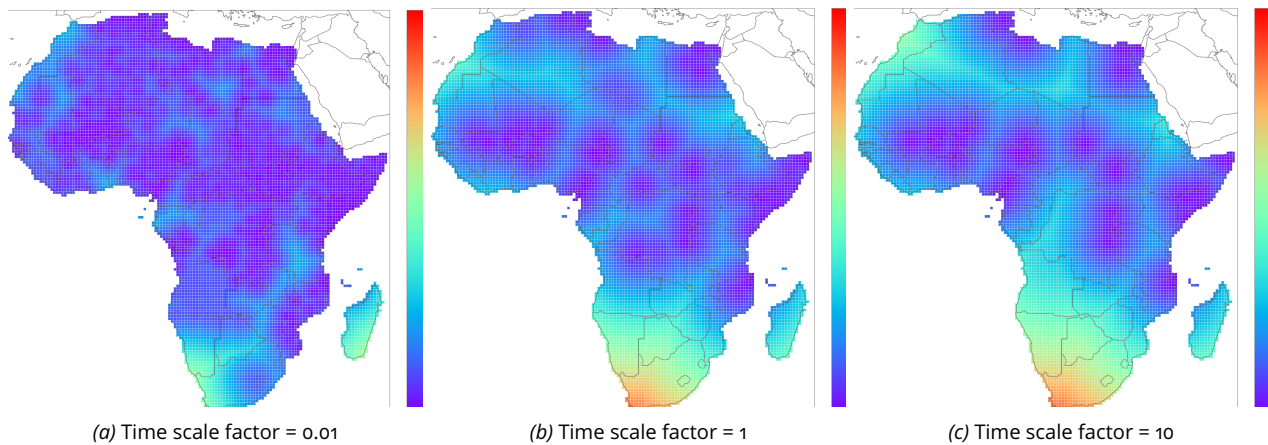
Estimation details

The model uses the 'one-step-ahead' approach (see Section C-2) and is estimated on data for Africa only.

Feature importances

The table below reports the feature importances for each type of violence and different time steps ($s = 1, 3, 6, 12, 24, 36$). Time distance is the most important feature to predict **sb** violence, slightly overcoming the importance of spatial lags. Spatial proximity to the outcome-specific violent is more relevant to predict **os** and **ns** violence.

Figure C-1. Maps illustrating scaling of the time dimension of the spacetime 'distance to event' feature.



| sb_sptime | 1 | 3 | 6 | 12 | 24 | 36 |
|-----------------------------|----------|----------|----------|----------|----------|----------|
| time_since_ged_dummy_sb | 0.107512 | 0.107484 | 0.123020 | 0.100964 | 0.094118 | 0.094741 |
| stdist_k1_t001_ged_dummy_sb | 0.105428 | 0.098914 | 0.088711 | 0.089833 | 0.083591 | 0.076906 |
| stdist_k1_t10_ged_dummy_sb | 0.096320 | 0.089038 | 0.080690 | 0.078302 | 0.072322 | 0.068418 |
| stdist_k1_t001_ged_dummy_ns | 0.094259 | 0.096035 | 0.097025 | 0.097669 | 0.101416 | 0.101881 |
| stdist_k1_t001_ged_dummy_os | 0.087747 | 0.092190 | 0.096659 | 0.095350 | 0.092889 | 0.087289 |
| time_since_ged_dummy_ns | 0.086342 | 0.090762 | 0.094679 | 0.101856 | 0.117246 | 0.121385 |
| stdist_k1_t1_ged_dummy_sb | 0.084704 | 0.079387 | 0.067897 | 0.074801 | 0.066150 | 0.062713 |
| stdist_k1_t10_ged_dummy_ns | 0.077513 | 0.078521 | 0.078629 | 0.078363 | 0.078601 | 0.079716 |
| stdist_k1_t1_ged_dummy_ns | 0.075472 | 0.077185 | 0.078402 | 0.079455 | 0.078083 | 0.079257 |
| time_since_ged_dummy_os | 0.066706 | 0.068698 | 0.072131 | 0.079068 | 0.088923 | 0.097605 |
| stdist_k1_t1_ged_dummy_os | 0.060491 | 0.063593 | 0.062384 | 0.063927 | 0.064310 | 0.065569 |
| stdist_k1_t10_ged_dummy_os | 0.057506 | 0.058193 | 0.059772 | 0.060412 | 0.062352 | 0.064519 |
| os_sptime | 1 | 3 | 6 | 12 | 24 | 36 |
| stdist_k1_t001_ged_dummy_ns | 0.112812 | 0.114766 | 0.115158 | 0.115528 | 0.115045 | 0.112240 |
| time_since_ged_dummy_ns | 0.109756 | 0.111741 | 0.110372 | 0.108476 | 0.107868 | 0.107639 |
| stdist_k1_t10_ged_dummy_ns | 0.100421 | 0.100341 | 0.100017 | 0.098784 | 0.096962 | 0.094419 |
| stdist_k1_t1_ged_dummy_ns | 0.093822 | 0.094733 | 0.095137 | 0.093507 | 0.093538 | 0.089860 |
| time_since_ged_dummy_os | 0.093048 | 0.090691 | 0.085692 | 0.084298 | 0.084892 | 0.087321 |
| time_since_ged_dummy_sb | 0.081286 | 0.083167 | 0.084491 | 0.086063 | 0.089744 | 0.092364 |
| stdist_k1_t001_ged_dummy_sb | 0.079351 | 0.083042 | 0.085573 | 0.088174 | 0.086615 | 0.087632 |
| stdist_k1_t001_ged_dummy_os | 0.078056 | 0.075618 | 0.075214 | 0.074504 | 0.075406 | 0.076562 |
| stdist_k1_t10_ged_dummy_os | 0.067830 | 0.064476 | 0.065007 | 0.064119 | 0.064749 | 0.065973 |
| stdist_k1_t10_ged_dummy_sb | 0.064353 | 0.066450 | 0.066428 | 0.067369 | 0.066254 | 0.065090 |
| stdist_k1_t1_ged_dummy_os | 0.061382 | 0.054244 | 0.055631 | 0.055922 | 0.057189 | 0.059770 |
| stdist_k1_t1_ged_dummy_sb | 0.057883 | 0.060731 | 0.061282 | 0.063257 | 0.061738 | 0.061129 |
| ns_sptime | 1 | 3 | 6 | 12 | 24 | 36 |
| stdist_k1_t001_ged_dummy_sb | 0.109862 | 0.117961 | 0.119419 | 0.118146 | 0.116368 | 0.113810 |
| time_since_ged_dummy_ns | 0.106852 | 0.100830 | 0.098596 | 0.095580 | 0.092569 | 0.091319 |
| time_since_ged_dummy_sb | 0.088366 | 0.093323 | 0.094842 | 0.095905 | 0.098549 | 0.101799 |
| stdist_k1_t001_ged_dummy_ns | 0.086110 | 0.082499 | 0.081475 | 0.084789 | 0.084629 | 0.085001 |
| stdist_k1_t10_ged_dummy_ns | 0.086016 | 0.077823 | 0.078586 | 0.076756 | 0.077869 | 0.075872 |
| time_since_ged_dummy_os | 0.082231 | 0.080108 | 0.080875 | 0.081867 | 0.081638 | 0.085535 |
| stdist_k1_t10_ged_dummy_sb | 0.079340 | 0.078824 | 0.077734 | 0.076918 | 0.076755 | 0.077052 |
| stdist_k1_t001_ged_dummy_os | 0.079320 | 0.081461 | 0.082591 | 0.083248 | 0.084462 | 0.085120 |
| stdist_k1_t1_ged_dummy_sb | 0.077264 | 0.078349 | 0.077160 | 0.076874 | 0.076067 | 0.076416 |
| stdist_k1_t10_ged_dummy_os | 0.070087 | 0.071555 | 0.071920 | 0.071985 | 0.072631 | 0.071620 |
| stdist_k1_t1_ged_dummy_ns | 0.068134 | 0.068698 | 0.067232 | 0.069085 | 0.068662 | 0.068289 |
| stdist_k1_t1_ged_dummy_os | 0.066419 | 0.068568 | 0.069570 | 0.068848 | 0.069800 | 0.068167 |

Table C-5. Feature importances for the Spacetime model, **sb**, **os**, **ns**

Change history

The model has been in use since r.2020.02.01

C-3.3 Onset (onset24_1_all, onset24_100_all)

Description

The Onset models are run for two dependent outcomes: at least one BRD and at least 100 BRDs. An onset is defined as the first time a specific grid, or its neighbors, reached the threshold in a 24-month sliding window. Uses the features from the *all* model.

Estimation details

The model uses the 'one-step-ahead' approach (see Section C-2) and is estimated on data for Africa only.

Change history

The model has been in use since r.2020.02.01

Feature importances

The tables report the feature importance for each type of violence and different time steps ($s = 1, 3, 6, 12, 24, 36$). Please note that for broad models such as *Onset*, the tables include only the first 25 most important features. Spatial proximity to conflict episodes is the most important feature to predict any type of violence. The occurrence of **ns** violence in neighboring cells is especially important to forecast not only **ns** but also **sb** and **os** conflicts, suggesting that violent episodes which do not involve the state may be important to capture early signs of any type of violence. This may also indicate that **ns** violence can transition into other forms of more structured conflict such as **sb** violence. This suggests that the spatial setting is particularly relevant to predict violence at the *pgm* level, while the time dimension is more relevant to predict conflict at the *cm* level. Likewise, geographical context and climate-related factors are among the most important features to predict the outbreak of any violence types, including the type of land, the presence of natural resources and the value of the SPEI indicator of drought. This indicates that environmental-related factors may be relevant in predicting early signs of violence.

| sb_onset24_1_all | 1 | 3 | 6 | 12 | 24 | 36 |
|-----------------------------|----------|----------|----------|----------|----------|----------|
| stdist_k1_t001_ged_dummy_ns | 0.018598 | 0.018721 | 0.019086 | 0.019308 | 0.019544 | 0.019709 |
| stdist_k1_t10_ged_dummy_ns | 0.017685 | 0.017761 | 0.018193 | 0.018006 | 0.018319 | 0.018306 |
| stdist_k1_t1_ged_dummy_ns | 0.017220 | 0.017960 | 0.018163 | 0.018048 | 0.017681 | 0.018208 |
| stdist_k1_t001_ged_dummy_os | 0.016927 | 0.017356 | 0.017359 | 0.017737 | 0.017745 | 0.018085 |
| stdist_k1_t001_ged_dummy_sb | 0.016277 | 0.016268 | 0.016250 | 0.016787 | 0.016938 | 0.017166 |
| ln_pgd_bdists3 | 0.015931 | 0.015588 | 0.014851 | 0.014816 | 0.014574 | 0.014939 |
| pgd_pasture_ih | 0.015563 | 0.015229 | 0.014878 | 0.014901 | 0.014745 | 0.015204 |
| ln_pgd_capdist | 0.015244 | 0.014526 | 0.014458 | 0.014412 | 0.014256 | 0.014485 |
| stdist_k1_t10_ged_dummy_os | 0.015195 | 0.016050 | 0.016572 | 0.016935 | 0.017351 | 0.017441 |
| ln_pgd_pop_gpw_sum | 0.015126 | 0.014356 | 0.014219 | 0.014106 | 0.014370 | 0.014472 |
| pgd_agri_ih | 0.014963 | 0.014717 | 0.014428 | 0.014192 | 0.014418 | 0.014798 |
| ln_pgd_ttime_mean | 0.014832 | 0.014141 | 0.013805 | 0.013750 | 0.013566 | 0.013806 |
| time_since_ged_dummy_sb | 0.014728 | 0.014370 | 0.014460 | 0.014247 | 0.014424 | 0.014048 |
| stdist_k1_t1_ged_dummy_os | 0.014727 | 0.015213 | 0.015657 | 0.016019 | 0.016382 | 0.016779 |
| spdist_pgd_diamsec | 0.013466 | 0.013040 | 0.012774 | 0.012652 | 0.012542 | 0.012943 |
| time_since_ged_dummy_os | 0.013093 | 0.013086 | 0.013308 | 0.013211 | 0.013539 | 0.013389 |
| stdist_k1_t10_ged_dummy_sb | 0.012884 | 0.013566 | 0.014547 | 0.014563 | 0.015680 | 0.015639 |
| spei_1 | 0.012626 | 0.013553 | 0.013445 | 0.013604 | 0.013327 | 0.013359 |
| time_since_ged_dummy_ns | 0.012469 | 0.012495 | 0.012934 | 0.012734 | 0.013034 | 0.013307 |
| spdist_pgd_petroleum | 0.012393 | 0.011829 | 0.011702 | 0.011893 | 0.011783 | 0.012000 |
| spei_3 | 0.012196 | 0.012435 | 0.012801 | 0.012250 | 0.012301 | 0.012170 |
| spei_2 | 0.012189 | 0.012833 | 0.013094 | 0.012605 | 0.012520 | 0.012373 |
| stdist_k1_t1_ged_dummy_sb | 0.012178 | 0.012860 | 0.013540 | 0.014164 | 0.014570 | 0.014839 |
| spei_4 | 0.011924 | 0.011866 | 0.012170 | 0.012016 | 0.012287 | 0.011699 |
| pgd_urban_ih | 0.011408 | 0.010638 | 0.010445 | 0.010208 | 0.010243 | 0.010560 |

Table C-6. Feature importances for model onset_1, **sb**

| sb_onset24_100_all | 1 | 3 | 6 | 12 | 24 | 36 |
|-----------------------------|----------|----------|----------|----------|----------|----------|
| stdist_k1_t10_ged_dummy_ns | 0.017877 | 0.017514 | 0.018129 | 0.020543 | 0.020008 | 0.017569 |
| stdist_k1_t001_ged_dummy_ns | 0.017102 | 0.018185 | 0.018018 | 0.019094 | 0.018173 | 0.018612 |
| pgd_pasture_ih | 0.016470 | 0.016402 | 0.016078 | 0.015805 | 0.016246 | 0.017017 |
| stdist_k1_t1_ged_dummy_ns | 0.015509 | 0.016682 | 0.018007 | 0.017848 | 0.017159 | 0.018003 |
| ln_pgd_bdists3 | 0.015051 | 0.014315 | 0.013900 | 0.015072 | 0.014706 | 0.015503 |
| ln_pgd_capdist | 0.014640 | 0.014315 | 0.014673 | 0.014963 | 0.014792 | 0.015704 |
| pgd_agri_ih | 0.014068 | 0.014479 | 0.014350 | 0.014440 | 0.014700 | 0.015560 |
| ln_pgd_pop_gpw_sum | 0.014020 | 0.014417 | 0.014397 | 0.014337 | 0.014517 | 0.014947 |
| stdist_k1_t001_ged_dummy_os | 0.013946 | 0.014300 | 0.015245 | 0.015956 | 0.015676 | 0.017252 |
| ln_pgd_ttime_mean | 0.013921 | 0.013207 | 0.013155 | 0.013412 | 0.013235 | 0.013533 |
| spei_1 | 0.013277 | 0.014222 | 0.013672 | 0.012360 | 0.013622 | 0.013530 |
| spdist_pgd_diamsec | 0.013044 | 0.012635 | 0.013285 | 0.013635 | 0.013135 | 0.013921 |
| stdist_k1_t10_ged_dummy_os | 0.012700 | 0.013377 | 0.013427 | 0.014420 | 0.015592 | 0.015064 |
| spei_4 | 0.012019 | 0.011496 | 0.011588 | 0.011827 | 0.012595 | 0.011639 |
| spei_3 | 0.011621 | 0.012744 | 0.011888 | 0.011134 | 0.012547 | 0.011636 |
| stdist_k1_t1_ged_dummy_os | 0.011550 | 0.012980 | 0.012543 | 0.014200 | 0.015581 | 0.014892 |
| spei_2 | 0.011353 | 0.013514 | 0.012542 | 0.011936 | 0.011997 | 0.011857 |
| spei_6 | 0.011330 | 0.010791 | 0.011460 | 0.010913 | 0.012008 | 0.011833 |
| spei_5 | 0.011206 | 0.011146 | 0.011710 | 0.011362 | 0.012406 | 0.010976 |
| time_since_ged_dummy_ns | 0.011196 | 0.012099 | 0.011560 | 0.011931 | 0.011365 | 0.010927 |
| pgd_urban_ih | 0.011127 | 0.010970 | 0.010996 | 0.011480 | 0.011761 | 0.012236 |
| pgd_imr_mean | 0.011014 | 0.010794 | 0.010933 | 0.010974 | 0.010799 | 0.010717 |
| spei_10 | 0.010978 | 0.010597 | 0.010817 | 0.011544 | 0.011025 | 0.011504 |
| spdist_pgd_petroleum | 0.010891 | 0.011792 | 0.011100 | 0.011738 | 0.011543 | 0.012637 |
| spei_13 | 0.010791 | 0.010477 | 0.010717 | 0.010492 | 0.011404 | 0.011314 |

Table C-7. Feature importances for model onset_100, **sb**

| os_onset24_1_all | 1 | 3 | 6 | 12 | 24 | 36 |
|-----------------------------|----------|----------|----------|----------|----------|----------|
| stdist_k1_t10_ged_dummy_ns | 0.017171 | 0.016318 | 0.017487 | 0.017205 | 0.017446 | 0.017160 |
| stdist_k1_t001_ged_dummy_ns | 0.016921 | 0.017348 | 0.017808 | 0.017943 | 0.018247 | 0.018509 |
| stdist_k1_t001_ged_dummy_sb | 0.015953 | 0.016276 | 0.016427 | 0.016960 | 0.016857 | 0.017079 |
| stdist_k1_t1_ged_dummy_ns | 0.015642 | 0.015975 | 0.016532 | 0.017138 | 0.017108 | 0.016980 |
| stdist_k1_t001_ged_dummy_os | 0.015546 | 0.015717 | 0.016257 | 0.016751 | 0.016678 | 0.017493 |
| ln_pgd_pop_gpw_sum | 0.015359 | 0.014745 | 0.014216 | 0.014264 | 0.014335 | 0.014740 |
| ln_pgd_capdist | 0.015118 | 0.014728 | 0.014234 | 0.014150 | 0.013942 | 0.014311 |
| ln_pgd_bdist3 | 0.015080 | 0.014354 | 0.013812 | 0.013669 | 0.013650 | 0.013875 |
| pgd_agri_ih | 0.015041 | 0.014367 | 0.014001 | 0.014170 | 0.014514 | 0.014716 |
| pgd_pasture_ih | 0.014898 | 0.014120 | 0.013953 | 0.014173 | 0.014499 | 0.014584 |
| time_since_ged_dummy_os | 0.014462 | 0.013873 | 0.013720 | 0.013384 | 0.013084 | 0.012796 |
| stdist_k1_t10_ged_dummy_sb | 0.014218 | 0.014572 | 0.014590 | 0.014937 | 0.015457 | 0.015300 |
| ln_pgd_ttime_mean | 0.014214 | 0.013603 | 0.013253 | 0.013277 | 0.013054 | 0.013323 |
| stdist_k1_t1_ged_dummy_sb | 0.013287 | 0.013524 | 0.014255 | 0.014566 | 0.014513 | 0.014874 |
| spei_1 | 0.012986 | 0.013484 | 0.013943 | 0.013629 | 0.012821 | 0.013965 |
| spdist_pgd_petroleum | 0.012852 | 0.012306 | 0.012107 | 0.012077 | 0.011959 | 0.012242 |
| stdist_k1_t10_ged_dummy_os | 0.012631 | 0.013789 | 0.014424 | 0.014874 | 0.014921 | 0.015968 |
| time_since_ged_dummy_sb | 0.012562 | 0.012826 | 0.013079 | 0.012975 | 0.013047 | 0.013218 |
| time_since_ged_dummy_ns | 0.012295 | 0.012664 | 0.012622 | 0.012789 | 0.012656 | 0.012598 |
| spdist_pgd_diamsec | 0.012178 | 0.011893 | 0.011644 | 0.011554 | 0.011691 | 0.011959 |
| stdist_k1_t1_ged_dummy_os | 0.012072 | 0.012978 | 0.013369 | 0.014310 | 0.014310 | 0.015266 |
| spei_2 | 0.011998 | 0.013084 | 0.012996 | 0.012907 | 0.012758 | 0.013075 |
| spei_3 | 0.011972 | 0.012879 | 0.012238 | 0.012327 | 0.012225 | 0.012289 |
| pgd_urban_ih | 0.011914 | 0.011288 | 0.010594 | 0.010727 | 0.010679 | 0.010862 |
| pgd_savanna_ih | 0.011608 | 0.010884 | 0.010816 | 0.010794 | 0.010675 | 0.010918 |

Table C-8. Feature importances for model onset_1, **os**

| os_onset24_100_all | 1 | 3 | 6 | 12 | 24 | 36 |
|-----------------------------|----------|----------|----------|----------|----------|----------|
| stdist_k1_t10_ged_dummy_ns | 0.017445 | 0.016699 | 0.019595 | 0.016829 | 0.020981 | 0.019646 |
| ln_pgd_capdist | 0.016681 | 0.016653 | 0.017028 | 0.016816 | 0.017821 | 0.017378 |
| stdist_k1_t001_ged_dummy_ns | 0.016211 | 0.017199 | 0.017178 | 0.018765 | 0.018691 | 0.019507 |
| ln_pgd_bdist3 | 0.016001 | 0.015803 | 0.015389 | 0.015019 | 0.015042 | 0.014536 |
| stdist_k1_t1_ged_dummy_ns | 0.015875 | 0.016125 | 0.017777 | 0.016499 | 0.017971 | 0.018110 |
| pgd_pasture_ih | 0.015186 | 0.015188 | 0.015461 | 0.014780 | 0.015536 | 0.015304 |
| stdist_k1_t001_ged_dummy_sb | 0.014311 | 0.015115 | 0.016156 | 0.016099 | 0.016511 | 0.016749 |
| spdist_pgd_petroleum | 0.014217 | 0.013745 | 0.013762 | 0.013586 | 0.014029 | 0.014032 |
| pgd_agri_ih | 0.014016 | 0.014361 | 0.014899 | 0.014500 | 0.015111 | 0.015141 |
| ln_pgd_pop_gpw_sum | 0.013901 | 0.014202 | 0.014266 | 0.013925 | 0.014927 | 0.015349 |
| pgd_forest_ih | 0.013655 | 0.012587 | 0.012459 | 0.012613 | 0.013375 | 0.012820 |
| stdist_k1_t10_ged_dummy_sb | 0.013006 | 0.013660 | 0.014266 | 0.014295 | 0.015172 | 0.016371 |
| ln_pgd_ttime_mean | 0.012962 | 0.013216 | 0.013235 | 0.013528 | 0.013421 | 0.013696 |
| spei_1 | 0.012480 | 0.012381 | 0.014132 | 0.013508 | 0.013455 | 0.013442 |
| spei_3 | 0.012243 | 0.011852 | 0.013150 | 0.011688 | 0.011228 | 0.012210 |
| stdist_k1_t1_ged_dummy_sb | 0.011943 | 0.012117 | 0.013121 | 0.013668 | 0.013829 | 0.014960 |
| spdist_pgd_diamsec | 0.011938 | 0.011380 | 0.010855 | 0.011311 | 0.011561 | 0.012129 |
| spei_5 | 0.011892 | 0.010904 | 0.011936 | 0.011066 | 0.011267 | 0.011635 |
| spei_7 | 0.011666 | 0.010222 | 0.011201 | 0.011722 | 0.011117 | 0.010862 |
| stdist_k1_t001_ged_dummy_os | 0.011517 | 0.012830 | 0.014735 | 0.016146 | 0.016341 | 0.017237 |
| time_since_ged_dummy_sb | 0.011388 | 0.011912 | 0.012362 | 0.012453 | 0.013403 | 0.013674 |
| spei_4 | 0.011371 | 0.010809 | 0.011440 | 0.011132 | 0.012242 | 0.011442 |
| spei_10 | 0.011309 | 0.010728 | 0.010777 | 0.010492 | 0.010347 | 0.011264 |
| spei_6 | 0.011200 | 0.010705 | 0.011270 | 0.010794 | 0.011379 | 0.011102 |
| spei_8 | 0.011190 | 0.011080 | 0.010974 | 0.011227 | 0.010830 | 0.010705 |

Table C-9. Feature importances for model onset_100, **os**

| ns_onset24_1_all | 1 | 3 | 6 | 12 | 24 | 36 |
|-----------------------------|----------|----------|----------|----------|----------|----------|
| stdist_k1_t001_ged_dummy_os | 0.017490 | 0.017397 | 0.017192 | 0.018048 | 0.018350 | 0.018232 |
| stdist_k1_t001_ged_dummy_ns | 0.017099 | 0.017095 | 0.017120 | 0.017401 | 0.018091 | 0.018627 |
| stdist_k1_t001_ged_dummy_sb | 0.016631 | 0.016601 | 0.017072 | 0.017141 | 0.017900 | 0.017852 |
| ln_pgd_pop_gpw_sum | 0.015234 | 0.014336 | 0.014073 | 0.013969 | 0.014579 | 0.014486 |
| time_since_ged_dummy_ns | 0.015202 | 0.014847 | 0.014601 | 0.014739 | 0.014185 | 0.014129 |
| stdist_k1_t10_ged_dummy_sb | 0.014849 | 0.015039 | 0.015171 | 0.015582 | 0.015653 | 0.016315 |
| pgd_pasture_ih | 0.014780 | 0.013997 | 0.013844 | 0.014053 | 0.014548 | 0.014745 |
| ln_pgd_bdist3 | 0.014778 | 0.013969 | 0.013706 | 0.013809 | 0.013899 | 0.014019 |
| pgd_agri_ih | 0.014634 | 0.014054 | 0.013576 | 0.013731 | 0.014412 | 0.014768 |
| stdist_k1_t1_ged_dummy_os | 0.014279 | 0.014857 | 0.014687 | 0.015218 | 0.015783 | 0.016090 |
| stdist_k1_t1_ged_dummy_sb | 0.014256 | 0.014400 | 0.014673 | 0.014963 | 0.015672 | 0.015760 |
| spei_1 | 0.014057 | 0.013138 | 0.013190 | 0.012961 | 0.013192 | 0.013146 |
| stdist_k1_t10_ged_dummy_os | 0.014048 | 0.014750 | 0.014969 | 0.015433 | 0.016152 | 0.016007 |
| stdist_k1_t10_ged_dummy_ns | 0.014019 | 0.014733 | 0.015603 | 0.015788 | 0.016845 | 0.017245 |
| ln_pgd_capdist | 0.013941 | 0.013157 | 0.013329 | 0.013262 | 0.013719 | 0.013665 |
| ln_pgd_ttime_mean | 0.013799 | 0.013291 | 0.012685 | 0.013087 | 0.013250 | 0.013380 |
| stdist_k1_t1_ged_dummy_ns | 0.013703 | 0.014095 | 0.014700 | 0.015260 | 0.016019 | 0.016566 |
| time_since_ged_dummy_os | 0.012725 | 0.012911 | 0.013239 | 0.013322 | 0.013095 | 0.013058 |
| spei_2 | 0.012713 | 0.012330 | 0.012039 | 0.012795 | 0.013007 | 0.012053 |
| spdist_pgd_diamsec | 0.012638 | 0.012340 | 0.012047 | 0.012215 | 0.012562 | 0.012550 |
| time_since_ged_dummy_sb | 0.012506 | 0.013015 | 0.012957 | 0.012949 | 0.013102 | 0.013068 |
| spdist_pgd_petroleum | 0.012287 | 0.011679 | 0.011411 | 0.011676 | 0.011873 | 0.011806 |
| spei_3 | 0.011783 | 0.011797 | 0.011842 | 0.012655 | 0.012221 | 0.011270 |
| spei_4 | 0.011476 | 0.011445 | 0.011618 | 0.012523 | 0.011732 | 0.011535 |
| spei_5 | 0.011156 | 0.011430 | 0.011329 | 0.012066 | 0.011529 | 0.010996 |

Table C-10. Feature importances for the onset_1 model, **ns**

| ns_onset24_100_all | 1 | 3 | 6 | 12 | 24 | 36 |
|-----------------------------|----------|----------|----------|----------|----------|----------|
| stdist_k1_t001_ged_dummy_os | 0.017630 | 0.016404 | 0.017484 | 0.016799 | 0.019009 | 0.019260 |
| pgd_pasture_ih | 0.017079 | 0.015784 | 0.015300 | 0.015925 | 0.017052 | 0.018078 |
| ln_pgd_capdist | 0.015788 | 0.013898 | 0.014944 | 0.013748 | 0.016458 | 0.016175 |
| stdist_k1_t10_ged_dummy_sb | 0.015688 | 0.016772 | 0.013790 | 0.015368 | 0.015932 | 0.016008 |
| stdist_k1_t001_ged_dummy_sb | 0.015664 | 0.015934 | 0.016015 | 0.016979 | 0.017503 | 0.017469 |
| ln_pgd_bdist3 | 0.015645 | 0.014754 | 0.014990 | 0.014658 | 0.016136 | 0.016316 |
| stdist_k1_t001_ged_dummy_ns | 0.015445 | 0.016674 | 0.015411 | 0.016362 | 0.017385 | 0.019255 |
| stdist_k1_t1_ged_dummy_os | 0.015222 | 0.014107 | 0.014275 | 0.014156 | 0.015592 | 0.015142 |
| stdist_k1_t10_ged_dummy_os | 0.014695 | 0.013016 | 0.016443 | 0.013675 | 0.015059 | 0.014587 |
| stdist_k1_t10_ged_dummy_ns | 0.014687 | 0.014640 | 0.014056 | 0.014184 | 0.017644 | 0.020033 |
| ln_pgd_pop_gpw_sum | 0.014001 | 0.013293 | 0.013143 | 0.013729 | 0.015337 | 0.014278 |
| stdist_k1_t1_ged_dummy_ns | 0.013974 | 0.013230 | 0.014105 | 0.013697 | 0.015852 | 0.016030 |
| spdist_pgd_diamsec | 0.013754 | 0.013375 | 0.012657 | 0.013276 | 0.014618 | 0.014444 |
| pgd_agri_ih | 0.013275 | 0.012720 | 0.013183 | 0.013798 | 0.015252 | 0.016437 |
| ln_pgd_ttime_mean | 0.013200 | 0.012339 | 0.011968 | 0.012370 | 0.012922 | 0.013395 |
| stdist_k1_t1_ged_dummy_sb | 0.013161 | 0.013813 | 0.014298 | 0.012923 | 0.015712 | 0.015142 |
| spei_4 | 0.012803 | 0.010187 | 0.011763 | 0.011516 | 0.011284 | 0.009066 |
| time_since_ged_dummy_ns | 0.012457 | 0.012048 | 0.011572 | 0.011520 | 0.010420 | 0.011226 |
| spei_5 | 0.012270 | 0.010680 | 0.010868 | 0.011328 | 0.011011 | 0.009865 |
| time_since_ged_dummy_sb | 0.011655 | 0.012158 | 0.011257 | 0.010658 | 0.011124 | 0.011639 |
| spei_8 | 0.011592 | 0.011490 | 0.010685 | 0.010605 | 0.010843 | 0.010661 |
| spei_1 | 0.011473 | 0.013267 | 0.011328 | 0.012519 | 0.015526 | 0.012030 |
| spei_3 | 0.011449 | 0.011675 | 0.012484 | 0.010901 | 0.011644 | 0.010076 |
| spei_9 | 0.011443 | 0.011023 | 0.011110 | 0.010896 | 0.010459 | 0.010363 |
| spei_7 | 0.011418 | 0.012154 | 0.010821 | 0.011796 | 0.010552 | 0.010657 |

Table C-11. Feature importances for the onset_100 model, **ns**

C-3.4 Natural geography (*pgd_natural*)

Description

The grid level natural geography model includes the spatial distance to diamonds and petroleum deposits. In fact, research has shown that the location of natural resources such as minerals and hydrocarbons play an important role in affecting the probability and duration of conflict, due to the opportunities and incentives it creates for rebel groups (Lujala, 2005). The model also contains indicators referring to the main land type: cultivated areas, barren, forest, mountains, svanna, shrub, pasture and urban areas. The type of land may affect the risk of conflict in two schematic ways; first, mountainous terrain offers an ideal setting for rebels to hide and fight (Fearon, 2003); second, arable, fertile lands may encourage deprived people to fight for seizing the resource (Hidalgo et al., 2010).

Estimation details

The model uses the 'one-step-ahead' approach (see Section C-2) and is estimated on data for Africa only.

Feature importances

The tables below report the feature importances for each type of violence and different time steps ($s = 1, 3, 6, 12, 24, 36$). The type of land and land use are the most important features to predict any type of violence at the *pgm* level. The availability of profitable natural resources such as diamond and petroleum are also relatively important in predicting conflict, although less than agricultural-related variables.

| <i>sb_pgd_natural</i> | 1 | 3 | 6 | 12 | 24 | 36 |
|-----------------------------|----------|----------|----------|----------|----------|----------|
| <i>pgd_pasture_ih</i> | 0.186816 | 0.185835 | 0.184290 | 0.185486 | 0.182741 | 0.180676 |
| <i>pgd_agri_ih</i> | 0.167282 | 0.168836 | 0.168543 | 0.170958 | 0.174737 | 0.177455 |
| <i>pgd_savanna_ih</i> | 0.131608 | 0.130035 | 0.130735 | 0.128957 | 0.128530 | 0.126468 |
| <i>pgd_forest_ih</i> | 0.119029 | 0.117281 | 0.118641 | 0.115980 | 0.113359 | 0.111252 |
| <i>pgd_urban_ih</i> | 0.107489 | 0.108503 | 0.108658 | 0.110872 | 0.113624 | 0.116976 |
| <i>spdist_pgd_diamsec</i> | 0.077449 | 0.078355 | 0.078250 | 0.076679 | 0.076750 | 0.074341 |
| <i>spdist_pgd_petroleum</i> | 0.070585 | 0.071312 | 0.070267 | 0.069365 | 0.067015 | 0.066040 |
| <i>pgd_mountains_mean</i> | 0.060417 | 0.059164 | 0.058636 | 0.057457 | 0.055587 | 0.053299 |
| <i>pgd_shrub_ih</i> | 0.054167 | 0.055438 | 0.056488 | 0.058680 | 0.060591 | 0.065352 |
| <i>pgd_barren_ih</i> | 0.025160 | 0.025241 | 0.025494 | 0.025565 | 0.027065 | 0.028142 |
| <i>os_pgd_natural</i> | 1 | 3 | 6 | 12 | 24 | 36 |
| <i>pgd_pasture_ih</i> | 0.183822 | 0.179077 | 0.182034 | 0.181357 | 0.183577 | 0.187210 |
| <i>pgd_agri_ih</i> | 0.181070 | 0.181687 | 0.181193 | 0.183699 | 0.185448 | 0.186256 |
| <i>pgd_urban_ih</i> | 0.146354 | 0.146887 | 0.146047 | 0.145173 | 0.143767 | 0.142298 |
| <i>pgd_savanna_ih</i> | 0.127994 | 0.130804 | 0.128486 | 0.130554 | 0.131086 | 0.129931 |
| <i>pgd_forest_ih</i> | 0.105601 | 0.106859 | 0.106696 | 0.108127 | 0.108669 | 0.107498 |
| <i>spdist_pgd_petroleum</i> | 0.062052 | 0.061115 | 0.061823 | 0.061091 | 0.061040 | 0.063095 |
| <i>spdist_pgd_diamsec</i> | 0.053217 | 0.054172 | 0.055439 | 0.053238 | 0.054484 | 0.054258 |
| <i>pgd_barren_ih</i> | 0.051318 | 0.049931 | 0.049354 | 0.047853 | 0.046319 | 0.043922 |
| <i>pgd_mountains_mean</i> | 0.048376 | 0.048647 | 0.048635 | 0.047571 | 0.046205 | 0.045055 |
| <i>pgd_shrub_ih</i> | 0.040197 | 0.040820 | 0.040293 | 0.041338 | 0.039405 | 0.040479 |
| <i>ns_pgd_natural</i> | 1 | 3 | 6 | 12 | 24 | 36 |
| <i>pgd_pasture_ih</i> | 0.171874 | 0.170917 | 0.171462 | 0.175321 | 0.186234 | 0.189402 |
| <i>pgd_agri_ih</i> | 0.156985 | 0.158277 | 0.159376 | 0.159589 | 0.166675 | 0.167907 |
| <i>pgd_urban_ih</i> | 0.139961 | 0.142161 | 0.142807 | 0.142327 | 0.138348 | 0.136953 |
| <i>pgd_savanna_ih</i> | 0.117082 | 0.121270 | 0.120925 | 0.120535 | 0.121039 | 0.118961 |
| <i>pgd_forest_ih</i> | 0.114341 | 0.112620 | 0.113523 | 0.113052 | 0.106766 | 0.104710 |
| <i>pgd_mountains_mean</i> | 0.083464 | 0.081336 | 0.080100 | 0.077500 | 0.071491 | 0.067845 |
| <i>spdist_pgd_petroleum</i> | 0.060687 | 0.060967 | 0.059910 | 0.059129 | 0.057419 | 0.056478 |
| <i>spdist_pgd_diamsec</i> | 0.055932 | 0.055709 | 0.053864 | 0.054932 | 0.053980 | 0.053694 |
| <i>pgd_shrub_ih</i> | 0.050606 | 0.050776 | 0.052162 | 0.052317 | 0.054016 | 0.056466 |
| <i>pgd_barren_ih</i> | 0.049070 | 0.045967 | 0.045871 | 0.045298 | 0.044032 | 0.047584 |

Table C-12. Feature importances for model natural geography, **sb**, **os**, **ns**

Change history

The model has been in use since r.2020.02.01

C-3.5 Social geography (*pgd_social*)

Description

The grid level social geography model contains a set of human geography features that may affect conflict, such as the (logged) distance to the national border, the nearest urban center and the capital city (Collier and Hoeffler, 2002). As conflict is deeply influenced by the degree of development—to the point that it has been defined as *development in reverse* (Collier et al., 2003)—the model also includes proxies of development akin the logged grid-level population size, GDP, infant mortality rate and an indicator of the share of excluded ethnic groups in each cell.

Estimation details

The model uses the ‘one-step-ahead’ approach (see Section C-2) and is estimated on data for Africa only.

Feature importances

The tables below report the feature importances for each type of violence and different time steps ($s = 1, 3, 6, 12, 24, 36$). Population size and gross cell product are the most important features to predict any type of violence, and their influence remains constant over the time steps. Infant mortality rate is relatively more important to predict **ns** violence, while distance to the capital city is more relevant to the other types of conflict (**sb**, **os**).

| <i>sb_pgd_social</i> | 1 | 3 | 6 | 12 | 24 | 36 |
|----------------------------|----------|----------|----------|----------|----------|----------|
| <i>ln_pgd_pop_gpw_sum</i> | 0.359695 | 0.359046 | 0.360514 | 0.363542 | 0.370824 | 0.382364 |
| <i>pgd_gcp_mer</i> | 0.239964 | 0.239668 | 0.239571 | 0.240666 | 0.237039 | 0.230920 |
| <i>ln_pgd_capdist</i> | 0.101451 | 0.101760 | 0.101729 | 0.099645 | 0.096991 | 0.095909 |
| <i>ln_pgd_bdist3</i> | 0.097956 | 0.098165 | 0.097535 | 0.095225 | 0.093435 | 0.090468 |
| <i>ln_pgd_ttime_mean</i> | 0.095284 | 0.096109 | 0.094523 | 0.093705 | 0.090578 | 0.088147 |
| <i>pgd_imr_mean</i> | 0.091934 | 0.091676 | 0.091956 | 0.092296 | 0.094897 | 0.095399 |
| <i>greq_1_pgd_excluded</i> | 0.013716 | 0.013575 | 0.014172 | 0.014922 | 0.016235 | 0.016793 |
| <i>os_pgd_social</i> | 1 | 3 | 6 | 12 | 24 | 36 |
| <i>ln_pgd_pop_gpw_sum</i> | 0.437880 | 0.435807 | 0.431703 | 0.433201 | 0.429984 | 0.429416 |
| <i>pgd_gcp_mer</i> | 0.251570 | 0.253885 | 0.251193 | 0.253239 | 0.255931 | 0.254437 |
| <i>ln_pgd_capdist</i> | 0.082636 | 0.083257 | 0.085232 | 0.084385 | 0.084478 | 0.085307 |
| <i>pgd_imr_mean</i> | 0.073763 | 0.074185 | 0.077619 | 0.075317 | 0.076407 | 0.077824 |
| <i>ln_pgd_bdist3</i> | 0.064367 | 0.064574 | 0.064457 | 0.063951 | 0.063948 | 0.065249 |
| <i>ln_pgd_ttime_mean</i> | 0.062949 | 0.061638 | 0.062680 | 0.062702 | 0.062593 | 0.062397 |
| <i>greq_1_pgd_excluded</i> | 0.026834 | 0.026654 | 0.027115 | 0.027205 | 0.026659 | 0.025370 |
| <i>ns_pgd_social</i> | 1 | 3 | 6 | 12 | 24 | 36 |
| <i>ln_pgd_pop_gpw_sum</i> | 0.358971 | 0.361053 | 0.360526 | 0.374131 | 0.379946 | 0.397179 |
| <i>pgd_gcp_mer</i> | 0.286361 | 0.282628 | 0.283776 | 0.276408 | 0.283145 | 0.271006 |
| <i>pgd_imr_mean</i> | 0.076293 | 0.078422 | 0.076658 | 0.074843 | 0.072730 | 0.072527 |
| <i>ln_pgd_ttime_mean</i> | 0.074648 | 0.073601 | 0.076416 | 0.075244 | 0.072876 | 0.073298 |
| <i>ln_pgd_capdist</i> | 0.071577 | 0.070141 | 0.072063 | 0.068652 | 0.070395 | 0.068590 |
| <i>greq_1_pgd_excluded</i> | 0.066944 | 0.067168 | 0.066648 | 0.064186 | 0.055601 | 0.052179 |
| <i>ln_pgd_bdist3</i> | 0.065206 | 0.066988 | 0.063913 | 0.066536 | 0.065307 | 0.065221 |

Table C-13. Feature importances for the social geography model, **sb**, **os**, **ns**

Change history

The model has been in use since r.2020.02.01

C-3.6 SPEI (*spei_full*)

Description

The SPEI model refers to the Standardized Precipitation Evapotranspiration Index (SPEI) global drought monitor data. The fully specified model includes SPEI data to model all 48 time scales ($s = 1$ up to $s = 48$) (*spei_full*). Drought occurrence is likely to increase the incidence of conflict, especially in vulnerable communities which lack the resources to cope with the environmental shock (von Uexkull et al., 2016). The SPEI index is a commonly used measure of drought (Vincente-Serrano et al., 2010) and is computed from both precipitation and temperature data, which makes it more suitable to climatic drought monitoring than other indices such as the SPI. Since the index is based on a water balance, higher SPEI values correspond to greater availability of water, while lower values correspond to water scarcity. A subseted model containing SPEI time scales 1, 3, 12, 24, 36, and 48 together with the history model's features is also included (*speisubset_leghist*)

Estimation details

The model uses the 'one-step-ahead' approach (see Section C-2) and is estimated on data for Africa only.

Change history

The model has been in use since r.2020.02.01

Feature importances

The tables below report the feature importances for each type of violence and different time steps ($s = 1, 3, 6, 12, 24, 36$). The SPEI index is a dynamic index which can be computed at different time-scales, from 1 up to 48 months. SPEI index computed at short time scale (one and two months) are the most important features to predict violence of any type, followed by the SPEI value averaged across four years. Although this is not an indication of causality, the feature importances suggests that drought can have both short-term and long term.

| sb_spei_full | 1 | 3 | 6 | 12 | 24 | 36 |
|--------------|----------|----------|----------|----------|----------|----------|
| spei_1 | 0.024547 | 0.025041 | 0.024803 | 0.024773 | 0.024616 | 0.024869 |
| spei_2 | 0.023013 | 0.023240 | 0.023187 | 0.022973 | 0.022880 | 0.023335 |
| spei_48 | 0.022656 | 0.022896 | 0.022957 | 0.022965 | 0.023417 | 0.023061 |
| spei_3 | 0.022391 | 0.022301 | 0.022126 | 0.022136 | 0.022160 | 0.022372 |
| spei_4 | 0.021911 | 0.021656 | 0.021472 | 0.021629 | 0.021946 | 0.021942 |
| spei_5 | 0.021583 | 0.021445 | 0.021219 | 0.021278 | 0.021350 | 0.021455 |
| spei_13 | 0.021565 | 0.021438 | 0.021339 | 0.021030 | 0.021283 | 0.020823 |
| spei_47 | 0.021541 | 0.021801 | 0.021823 | 0.021730 | 0.022079 | 0.022056 |
| spei_12 | 0.021517 | 0.021372 | 0.021478 | 0.021317 | 0.021235 | 0.020897 |
| spei_11 | 0.021437 | 0.021333 | 0.021241 | 0.021268 | 0.021233 | 0.020993 |
| spei_6 | 0.021377 | 0.021280 | 0.021176 | 0.021065 | 0.020949 | 0.021299 |
| spei_14 | 0.021202 | 0.021103 | 0.020930 | 0.020892 | 0.021043 | 0.020791 |
| spei_7 | 0.021147 | 0.020837 | 0.020755 | 0.020872 | 0.020873 | 0.021153 |
| spei_10 | 0.021101 | 0.020969 | 0.021018 | 0.020963 | 0.021075 | 0.020826 |
| spei_8 | 0.021068 | 0.020903 | 0.020610 | 0.020770 | 0.020954 | 0.021014 |
| spei_15 | 0.021057 | 0.020921 | 0.020700 | 0.020638 | 0.020700 | 0.020670 |
| spei_46 | 0.020838 | 0.020892 | 0.021142 | 0.020914 | 0.021341 | 0.021173 |
| spei_9 | 0.020818 | 0.020930 | 0.020726 | 0.020787 | 0.020918 | 0.021058 |
| spei_36 | 0.020750 | 0.020649 | 0.020810 | 0.020611 | 0.020496 | 0.020765 |
| spei_16 | 0.020639 | 0.020628 | 0.020464 | 0.020544 | 0.020470 | 0.020382 |
| spei_17 | 0.020588 | 0.020348 | 0.020361 | 0.020406 | 0.020268 | 0.020240 |
| spei_24 | 0.020578 | 0.020742 | 0.020791 | 0.020985 | 0.020691 | 0.020480 |
| spei_22 | 0.020552 | 0.020183 | 0.020595 | 0.020676 | 0.020584 | 0.020263 |
| spei_23 | 0.020547 | 0.020531 | 0.020822 | 0.020750 | 0.020541 | 0.020502 |
| spei_37 | 0.020537 | 0.020612 | 0.020851 | 0.020801 | 0.020545 | 0.020604 |

Table C-14. Feature importances for the Spei model, **sb**

| os_spei_full | 1 | 3 | 6 | 12 | 24 | 36 |
|--------------|----------|----------|----------|----------|----------|----------|
| spei_1 | 0.025448 | 0.025100 | 0.024559 | 0.025051 | 0.024332 | 0.026255 |
| spei_2 | 0.023646 | 0.023565 | 0.022834 | 0.023783 | 0.023077 | 0.023893 |
| spei_48 | 0.022752 | 0.023161 | 0.023183 | 0.023154 | 0.022578 | 0.022515 |
| spei_3 | 0.022516 | 0.022295 | 0.022009 | 0.022902 | 0.022754 | 0.023034 |
| spei_4 | 0.022256 | 0.021675 | 0.021346 | 0.022105 | 0.022230 | 0.022371 |
| spei_47 | 0.022005 | 0.021935 | 0.022010 | 0.022052 | 0.021678 | 0.021529 |
| spei_5 | 0.021603 | 0.021335 | 0.021107 | 0.021485 | 0.022031 | 0.022092 |
| spei_13 | 0.021557 | 0.021259 | 0.021400 | 0.020701 | 0.021352 | 0.020536 |
| spei_12 | 0.021413 | 0.021241 | 0.021476 | 0.021057 | 0.021246 | 0.021016 |
| spei_6 | 0.021316 | 0.020839 | 0.020996 | 0.020992 | 0.021393 | 0.021474 |
| spei_11 | 0.021225 | 0.021156 | 0.021105 | 0.020907 | 0.021313 | 0.021115 |
| spei_14 | 0.021204 | 0.021078 | 0.020968 | 0.020669 | 0.021344 | 0.020642 |
| spei_46 | 0.021118 | 0.021083 | 0.021240 | 0.021167 | 0.020869 | 0.020720 |
| spei_9 | 0.020963 | 0.020968 | 0.020833 | 0.020827 | 0.021181 | 0.021408 |
| spei_10 | 0.020864 | 0.020881 | 0.021014 | 0.020985 | 0.021441 | 0.020935 |
| spei_7 | 0.020852 | 0.020805 | 0.020707 | 0.020642 | 0.021360 | 0.021559 |
| spei_15 | 0.020851 | 0.020766 | 0.020743 | 0.020762 | 0.020987 | 0.020536 |
| spei_8 | 0.020844 | 0.020846 | 0.020918 | 0.020783 | 0.021086 | 0.021273 |
| spei_45 | 0.020616 | 0.020604 | 0.020714 | 0.020767 | 0.020799 | 0.020579 |
| spei_16 | 0.020590 | 0.020769 | 0.020542 | 0.020592 | 0.020848 | 0.020311 |
| spei_24 | 0.020578 | 0.020546 | 0.020934 | 0.020739 | 0.020094 | 0.020799 |
| spei_26 | 0.020496 | 0.020691 | 0.020765 | 0.020730 | 0.020078 | 0.020292 |
| spei_17 | 0.020452 | 0.020353 | 0.020318 | 0.020706 | 0.020659 | 0.020560 |
| spei_27 | 0.020449 | 0.020741 | 0.021065 | 0.020744 | 0.019807 | 0.020053 |
| spei_44 | 0.020431 | 0.020343 | 0.020253 | 0.020277 | 0.020319 | 0.020182 |

Table C-15. Feature importances for the Spei model, **os**

| ns_spei_full | 1 | 3 | 6 | 12 | 24 | 36 |
|--------------|----------|----------|----------|----------|----------|----------|
| spei_1 | 0.025039 | 0.024984 | 0.024143 | 0.023927 | 0.023880 | 0.024623 |
| spei_2 | 0.023432 | 0.023477 | 0.023069 | 0.023142 | 0.022814 | 0.023150 |
| spei_48 | 0.022931 | 0.022348 | 0.022762 | 0.023218 | 0.023332 | 0.021694 |
| spei_3 | 0.022300 | 0.022481 | 0.022225 | 0.022424 | 0.022727 | 0.022376 |
| spei_5 | 0.021875 | 0.021751 | 0.021130 | 0.021781 | 0.022008 | 0.021540 |
| spei_7 | 0.021658 | 0.021254 | 0.020635 | 0.021540 | 0.021372 | 0.021397 |
| spei_4 | 0.021574 | 0.021470 | 0.021568 | 0.021642 | 0.022146 | 0.021896 |
| spei_8 | 0.021529 | 0.021247 | 0.020709 | 0.021321 | 0.021434 | 0.021560 |
| spei_11 | 0.021444 | 0.020679 | 0.021244 | 0.021413 | 0.021163 | 0.021094 |
| spei_6 | 0.021355 | 0.022010 | 0.020983 | 0.021539 | 0.021483 | 0.021206 |
| spei_47 | 0.021340 | 0.021228 | 0.021338 | 0.021962 | 0.021985 | 0.020797 |
| spei_10 | 0.021308 | 0.020654 | 0.020965 | 0.021645 | 0.021248 | 0.021251 |
| spei_9 | 0.021226 | 0.020897 | 0.020945 | 0.021445 | 0.021274 | 0.021378 |
| spei_12 | 0.021032 | 0.021344 | 0.021606 | 0.021511 | 0.021397 | 0.021150 |
| spei_13 | 0.020985 | 0.021296 | 0.021702 | 0.021008 | 0.021350 | 0.020685 |
| spei_14 | 0.020980 | 0.020991 | 0.021647 | 0.020851 | 0.020799 | 0.020806 |
| spei_46 | 0.020913 | 0.020538 | 0.020329 | 0.021150 | 0.021175 | 0.020287 |
| spei_23 | 0.020864 | 0.020549 | 0.021065 | 0.021237 | 0.020556 | 0.020945 |
| spei_21 | 0.020808 | 0.020581 | 0.020724 | 0.021233 | 0.020735 | 0.021043 |
| spei_16 | 0.020715 | 0.020873 | 0.021501 | 0.020882 | 0.020627 | 0.020617 |
| spei_17 | 0.020698 | 0.021281 | 0.021224 | 0.020787 | 0.020881 | 0.020551 |
| spei_18 | 0.020671 | 0.020888 | 0.020936 | 0.021019 | 0.020423 | 0.020403 |
| spei_24 | 0.020641 | 0.020672 | 0.021170 | 0.020937 | 0.020405 | 0.020727 |
| spei_19 | 0.020582 | 0.020958 | 0.020209 | 0.020786 | 0.020206 | 0.020568 |
| spei_20 | 0.020575 | 0.020604 | 0.020318 | 0.020919 | 0.020938 | 0.020814 |

Table C-16. Feature importances for the Spei model, **ns**

C-3.7 Dynasim (**ds_dummy**, **ds_25**)

Description

The Dynasim models are specified as the canonical *pgm* models in Hegre et al. (2019) and they include the endogenously simulated violence types, with the addition of a new outcome of at least 25 BRDs in a grid cell. Both variants of simulated outcomes are included.

Estimation details

The model uses the dynamic simulation model illustrated in (see Hegre et al., 2019) and is estimated on data for Africa only. The single-death and 25 BRDs models are simulated together to inform each other.

Change history

The model has been in use since r.2020.02.01

C-3.8 All Themes (**all_themes**)

Description

The All Themes models include all the outcome-specific thematic models, i.e. the Natural Geography, Social Geography, Demographic, as well as the outcome-specific sets of conflict history features. We also include the Institutional and Oil Rent model, which have been removed from the ensemble due to their poor performance but can still contribute to the general RF setup. In fact, the advantage of broad models like this is due to their ability to capture interactions between different features and thus take into adequate account the complex relationships, feedback and conditional factors that may all together make conflict more likely.

Estimation details

The model uses the 'one-step-ahead' approach (see Section C-2) and is estimated on data for Africa only.

Change history

The model has been in use since r.2020.02.01

Feature importances

The tables below report the feature importances for each type of violence and different time steps ($s = 1, 3, 6, 12, 24, 36$). Please note that for broad models like *all_themes*, the tables report only the first 25 most important features. Similarly to the trend observed at the *cm* level, the most important features to predict violence at the *pgm* level are those related to each outcome-specific conflict history. Land type and use are especially relevant to predict **os** and **ns**. Population size is also among the most important features to predict violence of any type.

| sb_allthemes | 1 | 3 | 6 | 12 | 24 | 36 |
|----------------------------------|----------|----------|----------|----------|----------|----------|
| decay_12_time_since_ged_dummy_sb | 0.099209 | 0.094488 | 0.099113 | 0.101902 | 0.101993 | 0.103407 |
| ttag_1_ged_dummy_sb | 0.045804 | 0.042179 | 0.041325 | 0.033777 | 0.021375 | 0.019716 |
| ttag_2_ged_dummy_sb | 0.040205 | 0.040595 | 0.034238 | 0.028400 | 0.023053 | 0.018418 |
| decay_12_time_since_ged_dummy_os | 0.036827 | 0.040734 | 0.044385 | 0.048703 | 0.053020 | 0.056226 |
| ttag_3_ged_dummy_sb | 0.034080 | 0.026570 | 0.032917 | 0.027193 | 0.024604 | 0.015232 |
| ttag_4_ged_dummy_sb | 0.030862 | 0.030819 | 0.026634 | 0.023300 | 0.020891 | 0.015122 |
| ttag_6_ged_dummy_sb | 0.027330 | 0.023795 | 0.025342 | 0.017765 | 0.014526 | 0.014466 |
| ttag_7_ged_dummy_sb | 0.025321 | 0.026431 | 0.022920 | 0.020138 | 0.013497 | 0.013724 |
| ln_pgd_pop_gpw_sum | 0.024481 | 0.024154 | 0.024079 | 0.024373 | 0.025550 | 0.027417 |
| ttag_5_ged_dummy_sb | 0.024219 | 0.027388 | 0.024543 | 0.020296 | 0.016707 | 0.015041 |
| pgd_agri_ih | 0.023875 | 0.023793 | 0.023632 | 0.024580 | 0.025200 | 0.026094 |
| ttag_9_ged_dummy_sb | 0.021505 | 0.021068 | 0.021115 | 0.019590 | 0.015197 | 0.012352 |
| pgd_pasture_ih | 0.021497 | 0.021110 | 0.020719 | 0.020664 | 0.021410 | 0.022828 |
| ttag_8_ged_dummy_sb | 0.021017 | 0.023561 | 0.019207 | 0.018002 | 0.014997 | 0.015787 |
| fvp_ssp2_edu_sec_15_24_prop | 0.020887 | 0.021132 | 0.023333 | 0.026306 | 0.033412 | 0.033882 |
| ln_fvp_timeindep | 0.020825 | 0.021266 | 0.022792 | 0.034416 | 0.037612 | 0.037417 |
| pgd_gcp_mer | 0.020526 | 0.020353 | 0.020092 | 0.020120 | 0.021065 | 0.022113 |
| ln_fvp_timesincepreindepwar | 0.019858 | 0.020096 | 0.021214 | 0.026958 | 0.032233 | 0.035233 |
| ln_pgd_ttime_mean | 0.019766 | 0.019367 | 0.018493 | 0.018180 | 0.018419 | 0.018807 |
| ln_pgd_bdist3 | 0.019479 | 0.018860 | 0.018240 | 0.017985 | 0.018091 | 0.018218 |
| ln_pgd_capdist | 0.018940 | 0.018531 | 0.018200 | 0.018558 | 0.019730 | 0.021258 |
| decay_12_time_since_ged_dummy_ns | 0.018788 | 0.020886 | 0.023508 | 0.026639 | 0.030859 | 0.034208 |
| ttag_10_ged_dummy_sb | 0.018759 | 0.018260 | 0.018098 | 0.018384 | 0.015761 | 0.010946 |
| fvp_ssp2_urban_share_iiasa | 0.018592 | 0.018404 | 0.019612 | 0.022095 | 0.022554 | 0.024419 |
| ttag_11_ged_dummy_sb | 0.018205 | 0.017407 | 0.018189 | 0.014488 | 0.014873 | 0.010524 |

Table C-17. Feature importances for the All_themes model, **sb**

| os_allthemes | 1 | 3 | 6 | 12 | 24 | 36 |
|------------------------------------|----------|----------|----------|----------|----------|----------|
| decay_12_time_since_ged_dummy_ns | 0.152481 | 0.154399 | 0.151617 | 0.153147 | 0.148890 | 0.140953 |
| decay_12_time_since_ged_dummy_os | 0.062788 | 0.068855 | 0.072782 | 0.076277 | 0.077504 | 0.079672 |
| decay_12_time_since_ged_dummy_sb | 0.052166 | 0.058146 | 0.062706 | 0.068009 | 0.074263 | 0.076117 |
| decay_12_time_since_acled_dummy_pr | 0.051206 | 0.055557 | 0.059492 | 0.060714 | 0.063938 | 0.068115 |
| ttag_1_splag_1_1_ged_dummy_ns | 0.043436 | 0.040343 | 0.038555 | 0.038965 | 0.036988 | 0.036046 |
| ttag_1_ged_dummy_ns | 0.040614 | 0.033263 | 0.030270 | 0.025602 | 0.020571 | 0.016812 |
| ln_pgd_pop_gpw_sum | 0.028577 | 0.027418 | 0.026561 | 0.026806 | 0.026588 | 0.027284 |
| pgd_pasture_ih | 0.025929 | 0.024793 | 0.024375 | 0.024872 | 0.024916 | 0.026469 |
| pgd_agri_ih | 0.025543 | 0.024306 | 0.023993 | 0.024325 | 0.024988 | 0.026333 |
| pgd_gcp_mer | 0.025513 | 0.024362 | 0.023496 | 0.023192 | 0.023593 | 0.022399 |
| pgd_urban_ih | 0.024430 | 0.023837 | 0.023034 | 0.023209 | 0.023089 | 0.023579 |
| ln_pgd_ttime_mean | 0.021234 | 0.019680 | 0.019121 | 0.018783 | 0.018656 | 0.018616 |
| ln_pgd_capdist | 0.021189 | 0.020126 | 0.019786 | 0.019697 | 0.019486 | 0.019535 |
| ln_pgd_bdist3 | 0.020630 | 0.019954 | 0.019052 | 0.019133 | 0.018731 | 0.018866 |
| ln_fvp_population200 | 0.020579 | 0.020351 | 0.020711 | 0.020821 | 0.022059 | 0.022540 |
| ln_fvp_timesinceregimechange | 0.020168 | 0.022718 | 0.023282 | 0.022298 | 0.021005 | 0.019978 |
| ln_fvp_timesincepreindepar | 0.020143 | 0.020597 | 0.021190 | 0.019551 | 0.020924 | 0.021198 |
| ln_fvp_timeindep | 0.020046 | 0.020187 | 0.019514 | 0.019083 | 0.019722 | 0.019761 |
| fvp_ssp2_urban_share_iiasa | 0.019985 | 0.019025 | 0.019269 | 0.018713 | 0.019212 | 0.019446 |
| fvp_ssp2_edu_sec_15_24_prop | 0.019962 | 0.019214 | 0.019294 | 0.018458 | 0.018358 | 0.018306 |
| fvp_lngdpcap_nonoilrent | 0.019481 | 0.019018 | 0.018403 | 0.019134 | 0.022884 | 0.024924 |
| ttag_1_splag_1_1_acled_dummy_pr | 0.019043 | 0.018892 | 0.019819 | 0.020099 | 0.021198 | 0.020521 |
| spdist_pgd_diamsec | 0.018742 | 0.017795 | 0.017330 | 0.016642 | 0.016623 | 0.016910 |
| pgd_savanna_ih | 0.017465 | 0.016637 | 0.016467 | 0.016710 | 0.017060 | 0.017983 |
| spdist_pgd_petroleum | 0.017351 | 0.016241 | 0.016057 | 0.016033 | 0.015456 | 0.015735 |

Table C-18. Feature importances for the All_themes model, **os**

| ns_allthemes | 1 | 3 | 6 | 12 | 24 | 36 |
|------------------------------------|----------|----------|----------|----------|----------|----------|
| decay_12_time_since_ged_dummy_ns | 0.091485 | 0.093564 | 0.096816 | 0.104425 | 0.107150 | 0.107883 |
| decay_12_time_since_ged_dummy_os | 0.050372 | 0.059655 | 0.064912 | 0.073138 | 0.075634 | 0.077771 |
| decay_12_time_since_ged_dummy_sb | 0.043207 | 0.049537 | 0.055706 | 0.063783 | 0.073248 | 0.074407 |
| decay_12_time_since_acled_dummy_pr | 0.038182 | 0.044118 | 0.049943 | 0.052971 | 0.056319 | 0.062063 |
| ln_pgd_pop_gpw_sum | 0.027875 | 0.026274 | 0.025245 | 0.025066 | 0.025025 | 0.025920 |
| pgd_pasture_ih | 0.026739 | 0.024736 | 0.023965 | 0.023680 | 0.023891 | 0.025019 |
| pgd_agri_ih | 0.026462 | 0.025107 | 0.024338 | 0.024196 | 0.024976 | 0.026226 |
| ttag_1_ged_dummy_ns | 0.024739 | 0.018435 | 0.016955 | 0.014378 | 0.009763 | 0.007853 |
| pgd_gcp_mer | 0.022803 | 0.021465 | 0.020526 | 0.019586 | 0.019332 | 0.019038 |
| ln_pgd_bdist3 | 0.022536 | 0.021309 | 0.020254 | 0.019279 | 0.018871 | 0.019347 |
| ln_pgd_ttime_mean | 0.022480 | 0.020761 | 0.019703 | 0.018495 | 0.018383 | 0.018236 |
| ln_pgd_capdist | 0.022265 | 0.021221 | 0.020380 | 0.020093 | 0.019648 | 0.019578 |
| pgd_urban_ih | 0.021541 | 0.020649 | 0.020289 | 0.020408 | 0.020569 | 0.021555 |
| ln_fvp_population200 | 0.020238 | 0.019905 | 0.020275 | 0.020611 | 0.021985 | 0.023309 |
| ttag_2_ged_dummy_ns | 0.020152 | 0.022000 | 0.015321 | 0.012933 | 0.010491 | 0.009440 |
| ln_fvp_timesincepreindepar | 0.019930 | 0.020255 | 0.019819 | 0.020023 | 0.020561 | 0.021169 |
| ttag_1_splag_1_1_ged_dummy_ns | 0.019852 | 0.019125 | 0.017172 | 0.020365 | 0.024215 | 0.024326 |
| spdist_pgd_diamsec | 0.019753 | 0.018257 | 0.017259 | 0.016703 | 0.016337 | 0.016469 |
| fvp_ssp2_edu_sec_15_24_prop | 0.019563 | 0.018824 | 0.018627 | 0.017663 | 0.018076 | 0.018598 |
| ttag_3_ged_dummy_ns | 0.019465 | 0.016909 | 0.016043 | 0.012241 | 0.009486 | 0.007542 |
| ln_fvp_timesinceregimechange | 0.019221 | 0.020828 | 0.023264 | 0.021604 | 0.019785 | 0.019485 |
| ttag_4_ged_dummy_ns | 0.019151 | 0.014512 | 0.015464 | 0.014020 | 0.009075 | 0.008537 |
| fvp_ssp2_urban_share_iiasa | 0.018698 | 0.018319 | 0.018021 | 0.018028 | 0.019041 | 0.019687 |
| ln_fvp_timeindep | 0.018418 | 0.017673 | 0.017478 | 0.017875 | 0.018727 | 0.019663 |
| spdist_pgd_petroleum | 0.018204 | 0.017182 | 0.016345 | 0.015742 | 0.015262 | 0.015412 |

Table C-19. Feature importances for the All_themes model, **ns**

C-3.9 Cross Level (crosslevel)

Description

The risk of conflict in a given area is affected by both sub-national and national factors. The cross-level model builds on this notion and allows the two spatial levels of analysis to inform each other.

Estimation details

The model is estimated by using the product of the predicted probabilities at the *cm* and *pgm* levels. Specifically, the product of the *xgb_model* at the *pgm* level and the *all_glob* model at the *cm* level is used.

Change history

The model has been in use since r.2020.02.01

C-3.10 XGBoost All (*xgb_all*)

Description

The XGBoost model is a Gradient Boosting Machine (GBM) model. The model uses the same feature set as the *all_themes* model described above, with the notable addition of fatality estimates and event counts for all *spacetime* elements described above.

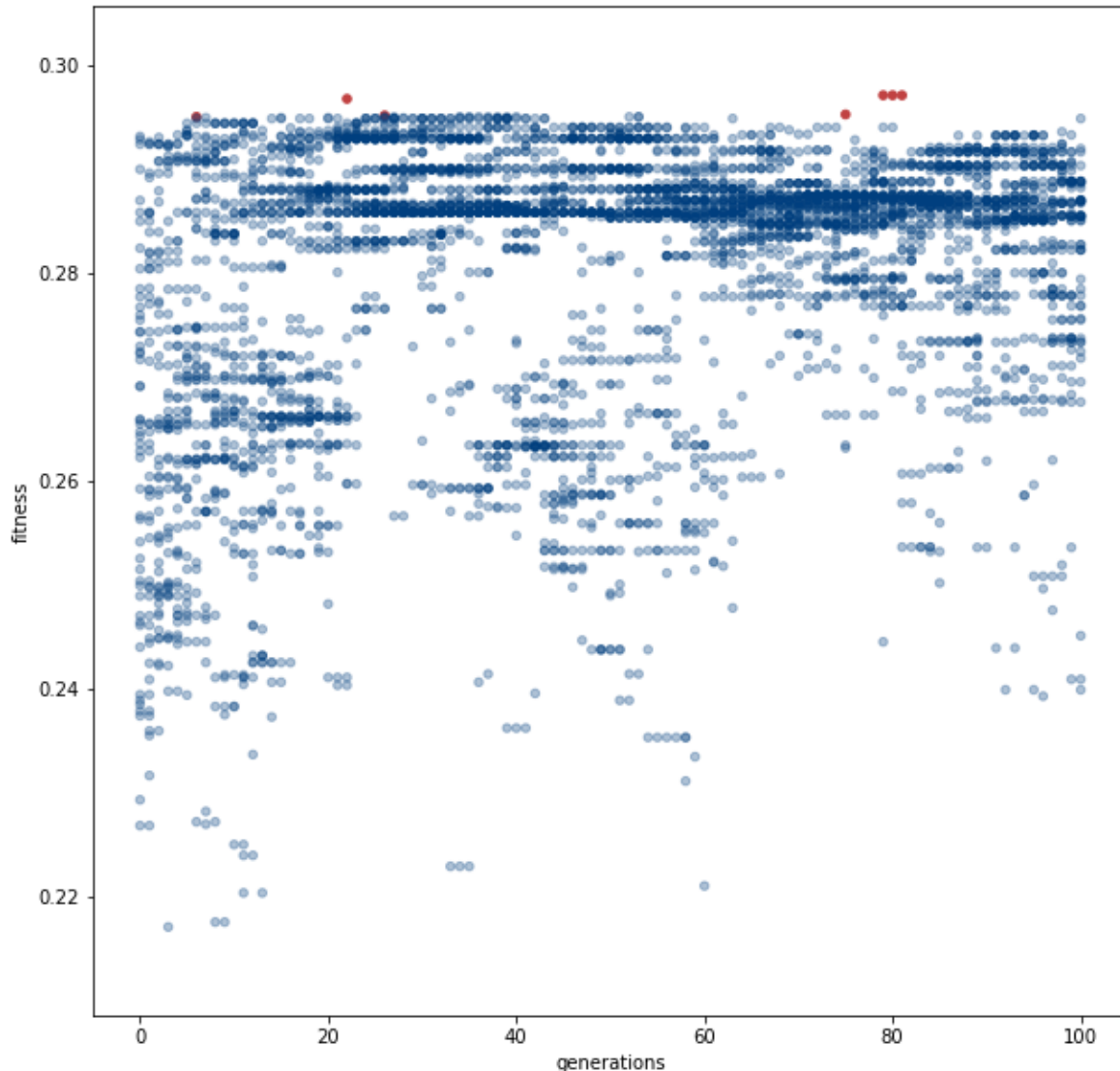
Estimation details

The model is estimated using the XGBoost algorithm (Chen and Guestrin, 2016), using both row and column sub-sampling as well as tree regularization. We performed hyper-parameter tuning on the following parameters: minimum loss reduction (or γ in XGB parlance), learning rate (or η in XGB parlance), maximum tree depth, minimum child weight and proportion of feature-space to sample (or column sample percentage per tree in XGB parlance). To prevent overfitting, common with boosted tree models, early stopping was implemented, with the model stopping the boosting procedure if the AUPR metric would not improve out-of-sample for 10 boosting iterations (see Appendix D for the reasoning behind AUPR as a metric). All out-of-sample evaluations were done on the subsequent partition of the data, in a similar manner with the rest of the ViEWS infrastructure. Hyper-parameters were tuned in the following manner:

1. A reasonable set of possible values were pre-selected for each hyper-parameter—resulting in a pool of 115,200 potential models.
2. The number of possible options, coupled with the size of the dataset, made it impossible to tune hyper-parameters exhaustively through grid-searching. Instead, for each constituent model, we optimized hyper-parameters through the use of a genetic algorithm (Russell and Norvig, 2016). This was applied in the following way: an initial sample of 50 possible hyper-parameter combinations were randomly sampled from the pool. 50 XGBoost models were trained with these hyper-parameters (using the 'train' partition), and scored based on the AUPR metric (out of sample, using the 'calibration' partition). 50 models were iterated across 100 generations. Figure C-2 shows the behavior of the 5,000 such estimated models across the 100 generations. Based on this score, models were allowed to probabilistically "mate", i.e., two high performing models will be merged taking some hyper-parameters (randomly) from the first the model and other hyper-parameters from the second model. 50 such mated "offspring" were produced. After this stage, some hyper-parameters were mutated from the mated "offspring", randomly being replaced with other hyper-parameters from the pool (with a probability of .1). Resulting models were then scored, and the mating and mutation procedure repeated for a total of 100 generations.
3. In order to avoid over-fitting of the hyper-parameter tuning routine on the calibration partition, we selected the best five performing hyper-parameter sets in any generation.

For each time-step in the infrastructure, an ensemble of five XGBoost models was trained, one with each set of hyper-parameters identified in the above procedure. A simple ensemble was constructed, taking the

Figure C-2. Performance (AUPR) of the genetic-optimized xgb models across the 100 generations of optimization. Each dot represents a model: the horizontal axis represents the generation where the model was produced, and the vertical axis the performance of that model. Note that the genetic algorithm was specified in such a way as to produce maximum variability as to increase the probability of identifying the best performing models.



simple average of predictions as the final prediction of the ensemble. As early stopping is required, the following solution was implemented:

- For models trained only on the 'train' partition, early stopping was done on 'calibration';
- For models trained on 'train' and 'calibrate' partitions, early stopping was done on the 'evaluate' partition;
- For models used for final forecasting, trained on all partitions, training ended at the last month with full UCDP data (currently December 2018); early stopping was done on data containing UCDP candidate events as targets (January 2019 - November 2019).

Note that hyper-parameter tuning is always done only once—with models trained on the 'train' partition and evaluated on the 'calibration' partition.

Figure C-3. Feature importances scores (in the gain domain) in a 6-month ahead state-based (sb) xgb model.

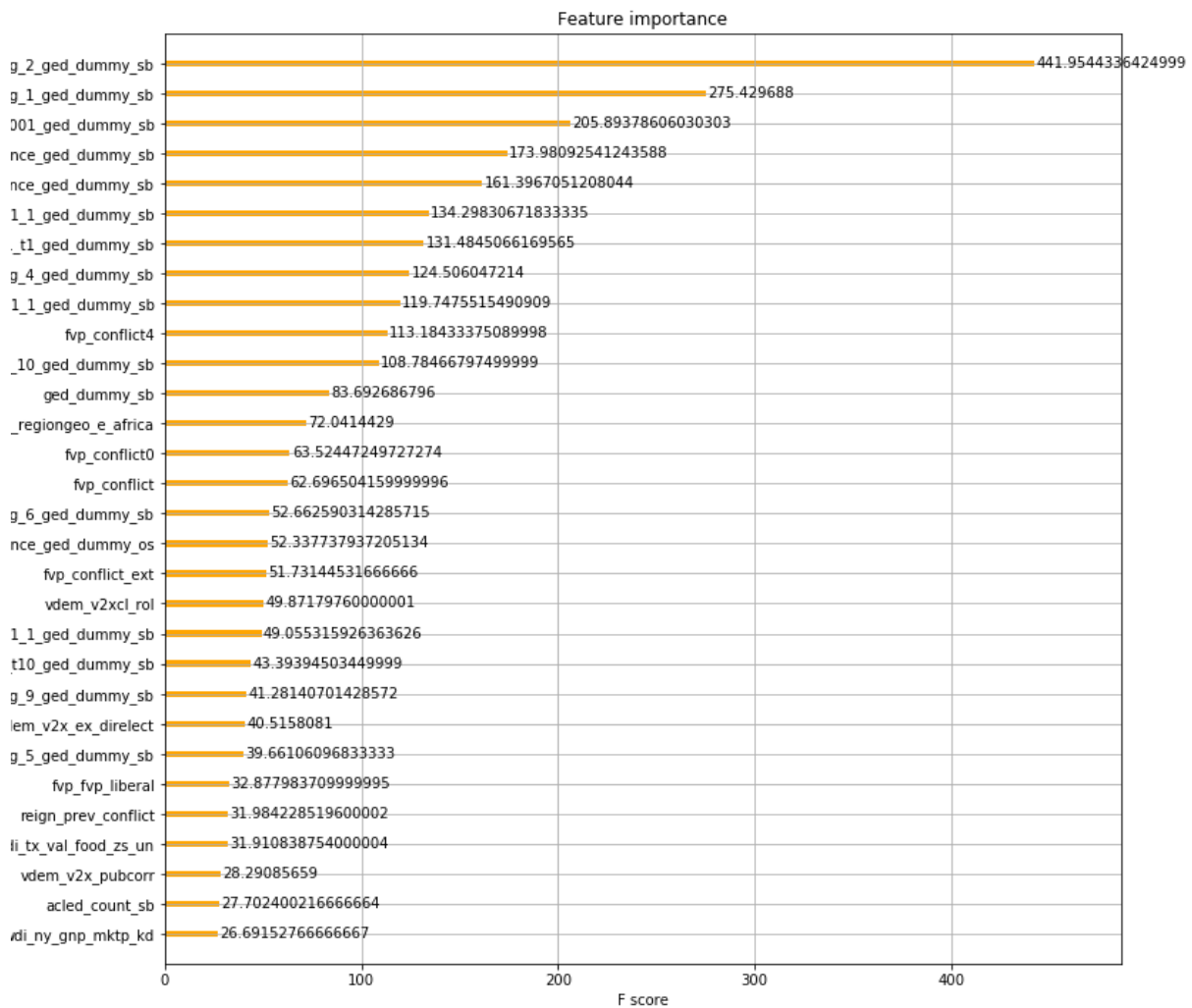


Figure C-3 shows feature importances scores for the most important 30 features from the xgb state-based (sb) 6-month ahead model in the gain domains (features that generate the highest total improvement in the F score).

Change history

The model has been in use since r.2020.02.01

C-4 CHANGES IN PGM MODELS

The *pgm* ensembles contain several broad models including all features mentioned below (a description of each *cm* model is reported in Appendix B). *Pgm* models are based on spatially disaggregated data, in line with recent empirical research which increasingly uses Geographical Information System (GIS) to investigate conflict at a sub-national level (Tollefsen, Strand, and Buhaug, 2012). Although *cm* models are especially useful for predictions of new conflicts, the higher spatial resolution of conflict predictors enable the *pgm* models to better capture differences across space that are leveled out by national average. Results of *pgm* models can not only contribute with new insight on the current empirical research on the causes of conflict,

but also provide a more thorough indication to policy-makers.

The new *pgm* models mainly include features which reflect recent empirical research findings, such as a drought model (*spei_full*). SPEI refers to the Standardized Precipitation Evapotranspiration Index, a commonly used measure of drought (Vicente-Serrano, Beguería, and López-Moreno, 2010). The SPEI index is computed from both precipitation and temperature data, which makes it more suitable to climatic drought monitoring than other indices. The model captures the non-linear relationship, featuring a higher risk of conflict at the two extremes of the scale, i.e. when SPEI is either higher or lower than average.

The *sptime* model focuses on the distance to conflict episodes both in space and time, by means of a single metric that measures the distance from a given grid-cell month to the most proximate conflict observation across both space and time. The model contains a number of these features representing various relative weightings of spatial and temporal distance. This model enables us to comprehensively account for the role of spatial and temporal context in affecting the probability of conflict (Buhaug and Rød, 2006; Raleigh and Hegre, 2009). Finally, three *pgm* models are trained using only onsets of conflict as the outcome to forecast.

C-5 DETAILED DESCRIPTIONS, CONSTITUENT MODELS

The following sections delve deeper into the three different types of violence (**sb**, **os**, **ns**) and present the results of predictions thereof.

C-5.1 State-based conflict (**sb**)

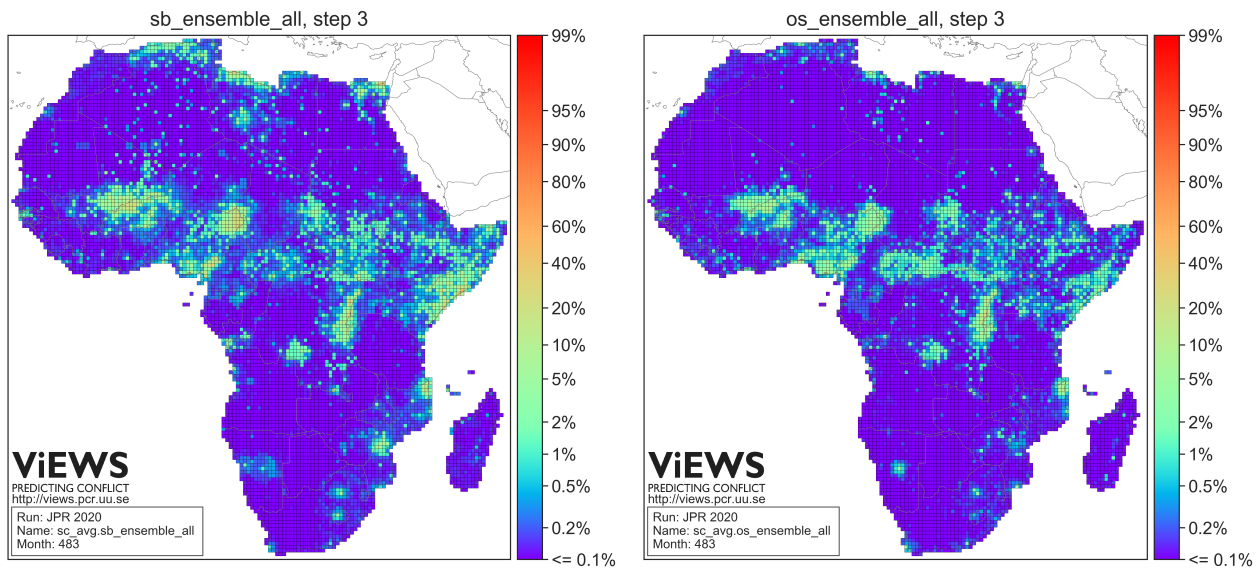
State-based violence is defined according to the standard UCPD definition, as a contested incompatibility that concerns government and/or territory where the use of armed force between two parties, of which at least one is the government of a state, results in at least 25 battle-related deaths in one calendar year (Pettersson and Eck, 2018). State-based conflicts are thus characterized by the use of the force by the government as an active side of conflict, as opposed to non-state conflicts where none of the active sides are a government. Predictions of these types of violence may be of interest for all scholars of civil wars and those concerned with the main drivers of conflict against the state. By contrast, the following sections may be more relevant for researchers of other forms of violence which do not involve the government as an active part.

As follows, we present the prediction maps at the grid-cell level (*pgm*) for **sb**.

Prediction maps, forecasts (**sb**)

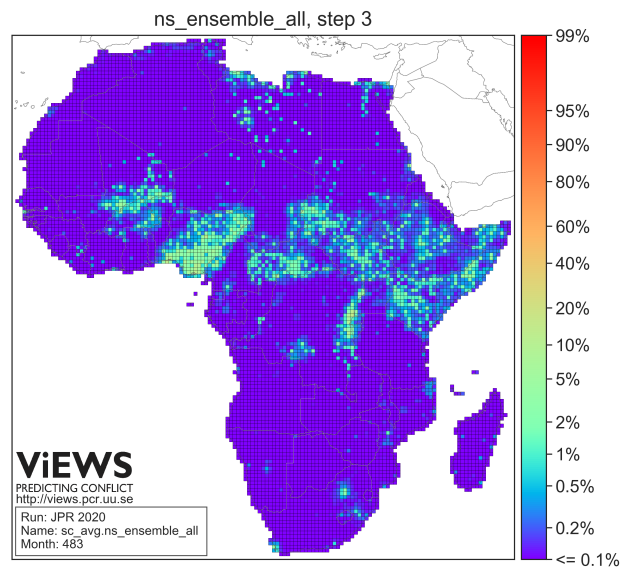
Figure C-5 shows the forecasts for the geographical *pgm* level for March 2020 based on the $s = 3$ model. All models are calibrated, i.e. rescaled using a logit procedure so that mean predicted probability in the calibration period is similar to the observed proportion of conflict. Models that separate poorly at this level has a bluish color, as the mean probability is much lower than for *cm*. Figure C-6 show the same for December 2022, i.e. $s = 36$ months into the future based on data up to and including December 2019.

Figure C-4. Predicted probabilities, ensemble models, **sb**, **os** and **ns**, $s = 3$ (month 483, March 2020), based on data up to December 2019



(a) Ensemble, **sb**

(b) Ensemble, **os**



(c) Ensemble, **ns**

Figure C-5. Predicted probabilities, constituent models, **sb**, $s = 3$ (month 483, March 2020), based on data up to December 2019

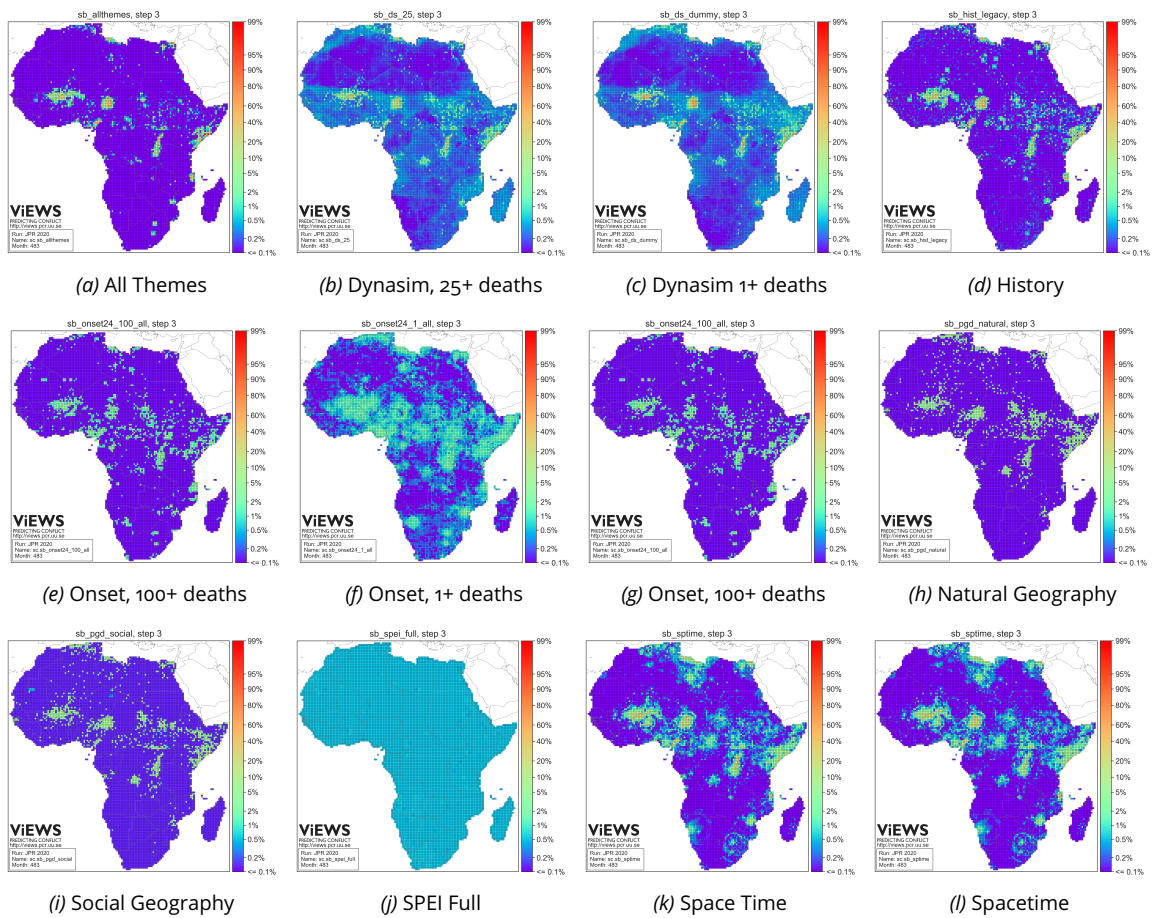
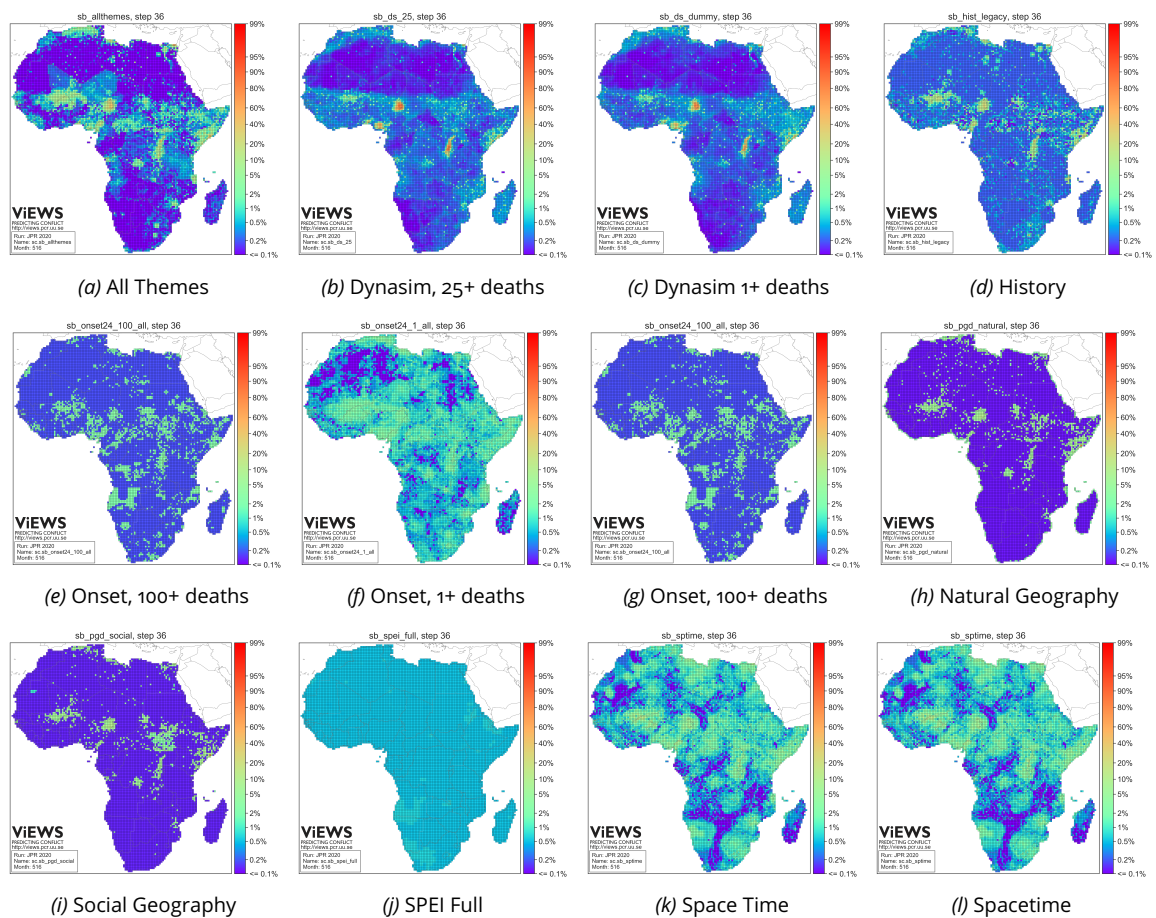


Figure C-6. Predicted probabilities, constituent models, **sb**, $s = 36$ (month 516, December 2022), based on data up to December 2019



C-5.2 One-sided violence (os)

One-sided violence is defined as the deliberate use of armed force by the government of a state or by a formally organized group against civilians which result in at least 25 BRDs in a year (Pettersson and Eck, 2018). Unlike state-based conflict, *os* violence involves the use of the armed force by one actor against the civilian population. Predictions of **os** can be of particular interest to scholars of atrocities and violence against civilians.

As follows, we present the prediction maps at the grid-cell level (*pgm*) for **os**.

Prediction maps, forecasts (os)

Figure C-5 shows the forecasts for the geographical *pgm* level for March 2020 based on the $s = 3$ model. All models are calibrated, i.e. rescaled using a logit procedure so that mean predicted probability in the calibration period is similar to the observed proportion of conflict. Models that separate poorly at this level has a blueish color, as the mean probability is much lower than for *cm*. Figure C-8 show the same for December 2022, i.e. $s = 36$ months into the future based on data up to and including December 2019.

Figure C-7. Predicted probabilities, constituent models, **os**, $s = 3$ (month 483, March 2020), based on data up to December 2019

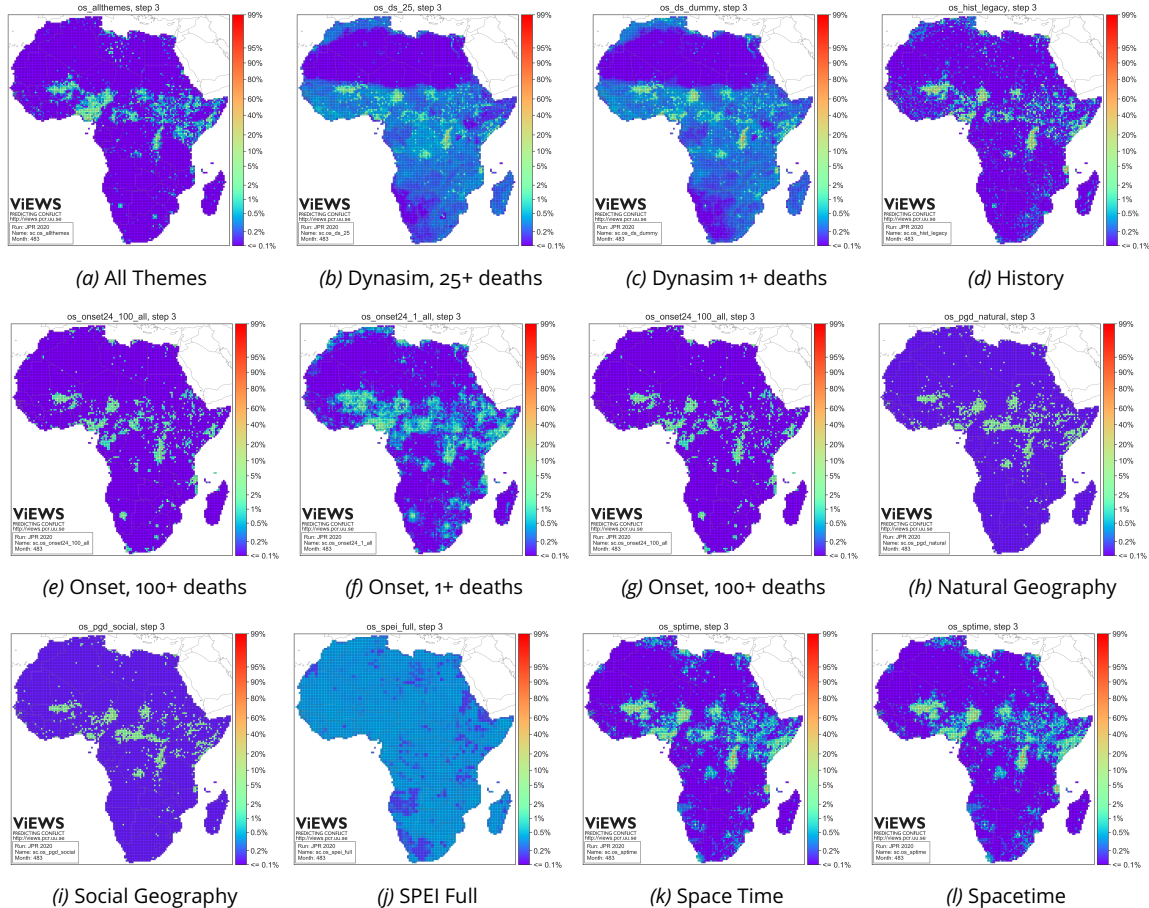
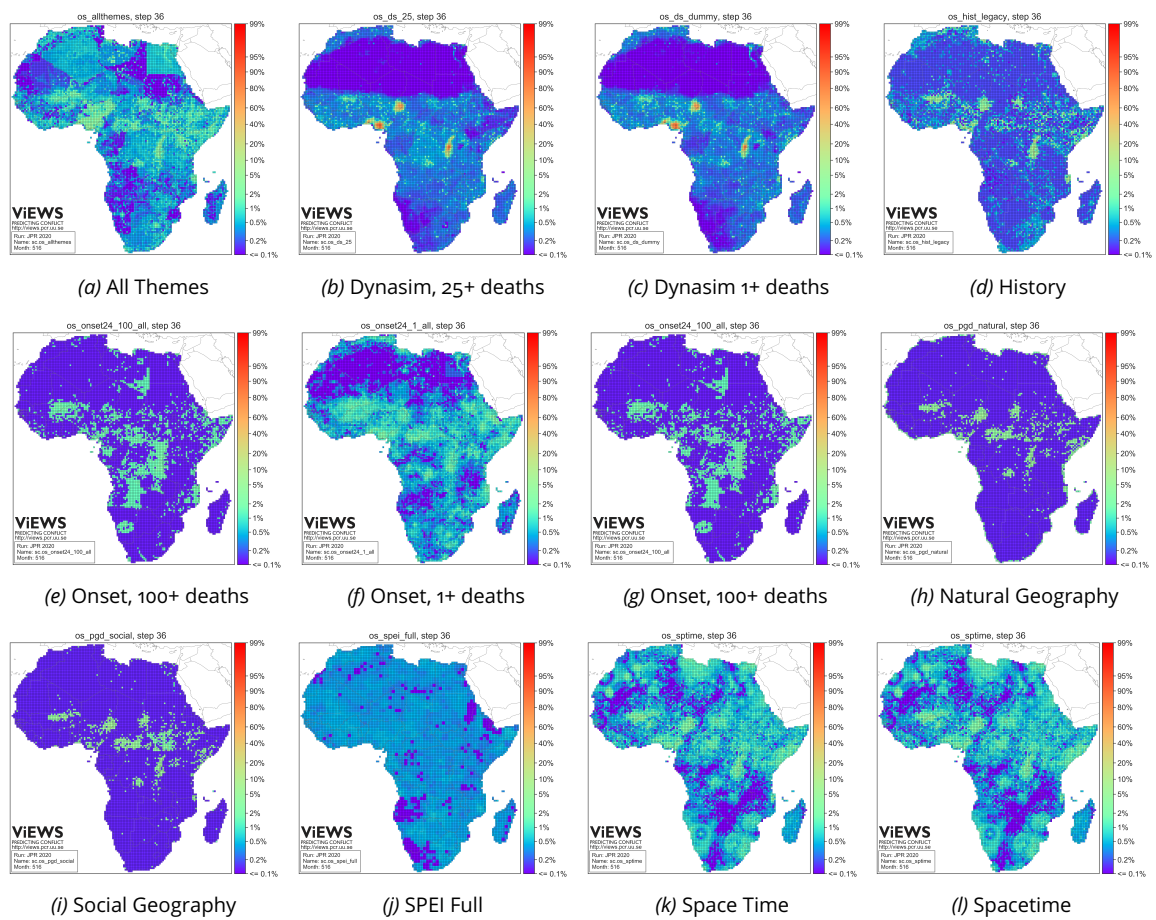


Figure C-8. Predicted probabilities, constituent models, **os**, $s = 36$ (month 516, December 2022), based on data up to December 2019



C-5.3 Non-state conflict (ns)

Non-state conflict is defined as the use of armed force by two formally organized groups, none of which is the government of a state, which result in at least 25 BRDs in a year (Pettersson and Eck, 2018). Conflicts between rebel or ethnic groups fall in this category.

As follows, we present the prediction maps for **ns**.

Prediction maps, forecasts (ns)

Figure C-9 shows the forecasts for the geographical *pgm* level for March 2020 based on the $s = 3$ model. All models are calibrated, i.e. re-scaled using a logit procedure so that mean predicted probability in the calibration period is similar to the observed proportion of conflict. Models that separate poorly at this level has a bluish color, as the mean probability is much lower than for *cm*. Figure C-10 show the same for December 2022, i.e. $s = 36$ months into the future based on data up to and including December 2019.

Figure C-9. Predicted probabilities, constituent models, **ns**, $s = 3$ (month 483, March 2020), based on data up to December 2019

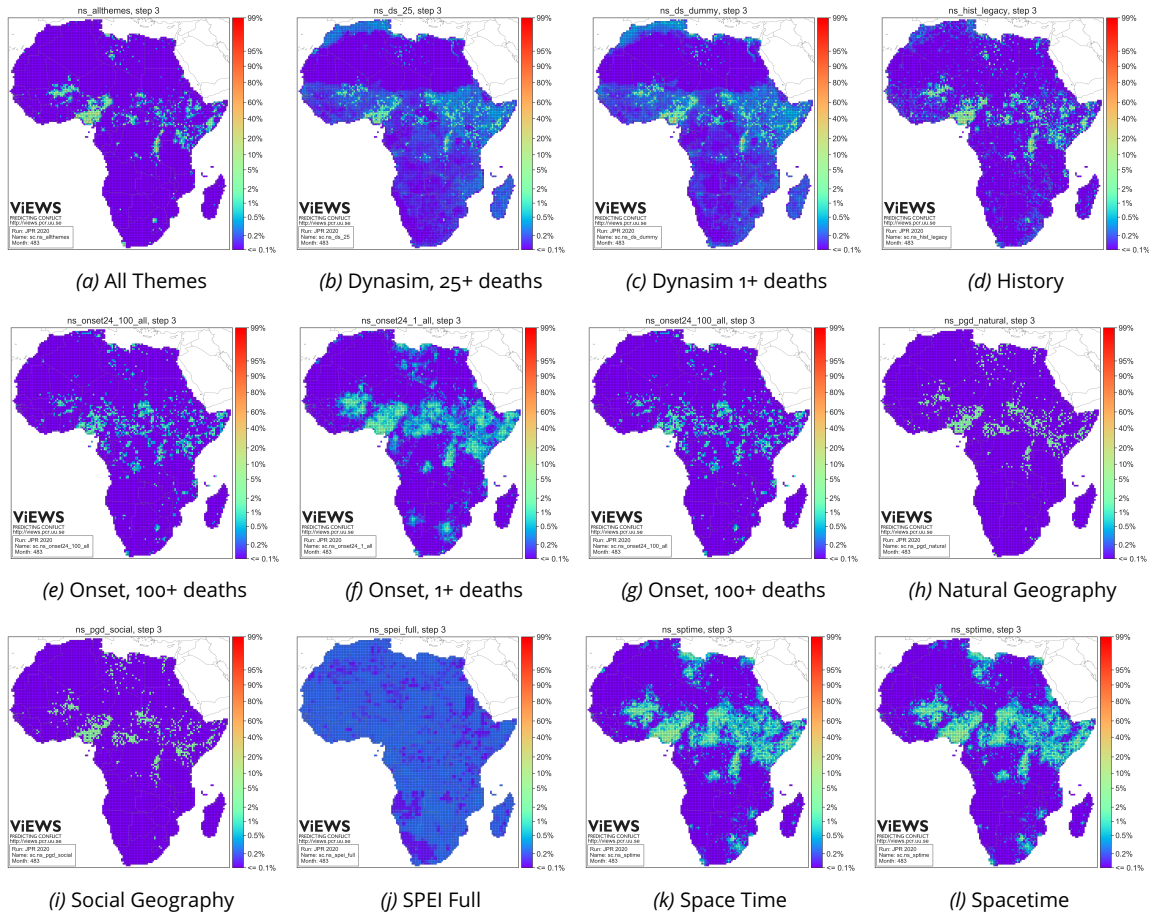
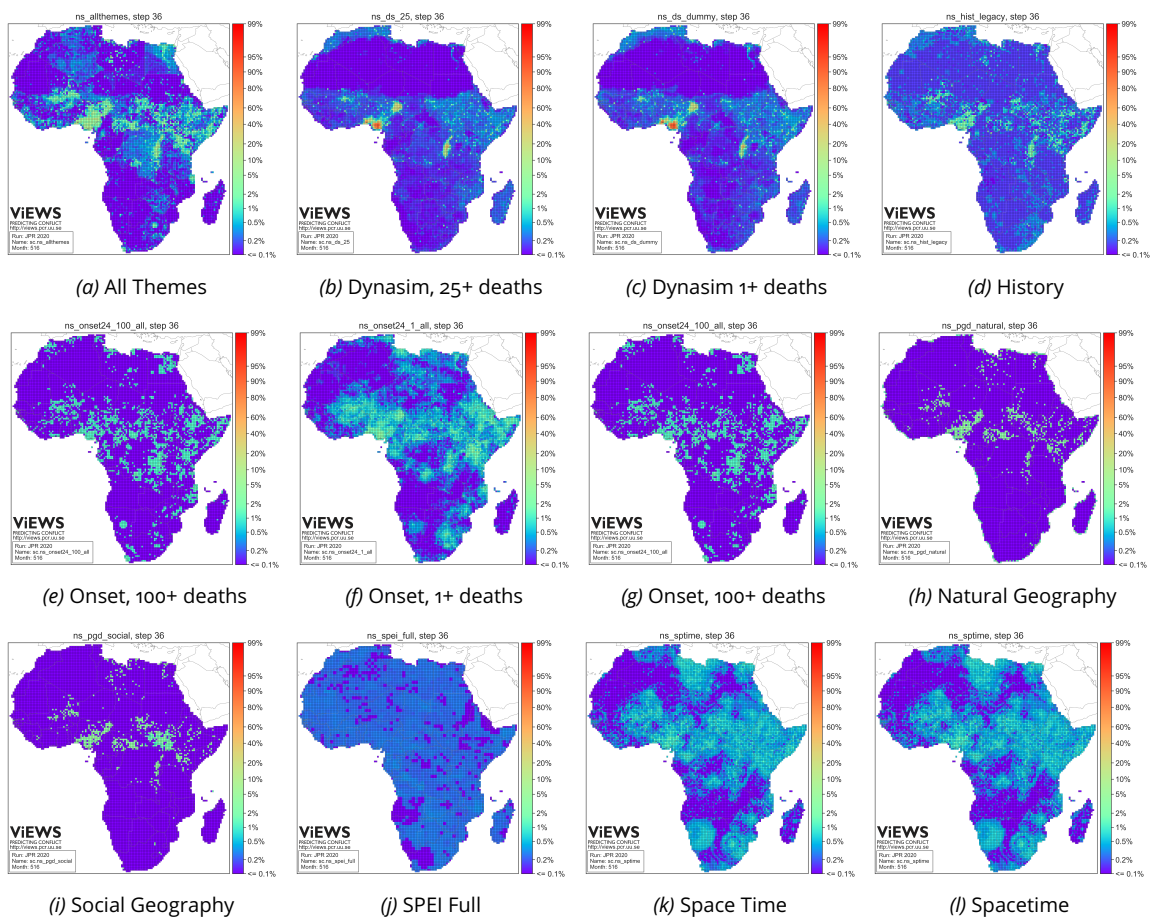


Figure C-10. Predicted probabilities, constituent models, *ns*, $s = 36$ (month 516, December 2022), based on data up to December 2019



REFERENCES

- Breiman, Leo (2001). "Random Forests". In: *Machine learning* 45.1, pp. 5–32.
- Buhaug, Halvard and Kristian Skrede Gleditsch (2008). "Contagion or Confusion? Why Conflicts Cluster in Space". In: *International Studies Quarterly* 52, pp. 215–233.
- Buhaug, Halvard and Jan K. Rød (2006). "Local Determinants of African Civil Wars, 1970–2001". In: *Political Geography* 25.3, pp. 315–335.
- Chen, Tianqi and Carlos Guestrin (2016). "Xgboost: A scalable tree boosting system". In: *Proceedings of the 22nd acm sigkdd international conference on knowledge discovery and data mining*, pp. 785–794.
- Collier, Paul, Lani Elliot, Håvard Hegre, Anke Hoeffler, Marta Reynal-Querol, and Nicholas Sambanis (2003). *Breaking the Conflict Trap. Civil War and Development Policy*. Oxford: Oxford University Press. URL: <https://openknowledge.worldbank.org/handle/10986/13938>.
- Collier, Paul, Håvard Hegre, and Arvid Raknerud (2003). *f War*.
- Collier, Paul and Anke Hoeffler (2002). "On the Incidence of Civil War in Africa". In: *Journal of Conflict Resolution* 46.1, pp. 13–28.
- Fearon, James D. (2003). "Presentation". In: *Workshop on Conflict Data*. Oslo.
- Friedman, Jerome H. (2001). "Greedy function approximation: a gradient boosting machine". In: *Annals of statistics*, pp. 1189–1232.
- Géron, Aurélien (2017). *Hands-on machine learning with Scikit-Learn and TensorFlow: concepts, tools, and techniques to build intelligent systems*. O'Reilly Media, Inc.
- Hegre, Håvard, Marie Allansson, Matthias Basedau, Mike Colaresi, Mihai Croicu, Hanne Fjelde, Frederick Hoyles, Lisa Hultman, Stina Högladh, Remco Jansen, Naima Mouhle, Sayeed Awn Muhammad, Desirée Nilsson, Håvard Mogleiv Nygård, Gudlaug Olafsdottir, Kristina Petrova, David Randahl, Espen Geelmuyden Rød, Gerald Schneider, Nina von Uexkull, and Jonas Vestby (2019). "ViEWS: A political Violence Early Warning System". In: *Journal of Peace Research* 56.2, pp. 155–174. URL: <https://doi.org/10.1177/0022343319823860>.
- Hegre, Håvard, Halvard Buhaug, Katherine V. Calvin, Jonas Nordkvelle, Stephanie T. Waldhoff, and Elisabeth Gilmore (2016). "Forecasting civil conflict along the shared socioeconomic pathways". In: *Environmental Research Letters* 11.5, p. 054002. DOI: 10.188/1748-9326/11/5/054002.
- Hegre, Håvard, Joakim Karlsen, Håvard Mogleiv Nygård, Håvard Strand, and Henrik Urdal (2013). "Predicting Armed Conflict 2010–2050". In: *International Studies Quarterly* 57.2, pp. 250–270. DOI: 10.1111/isqu.12007.
- Hidalgo, F. Daniel, Suresh Naidu, Simeon Nichter, and Neal Richardson (2010). "Economic Determinants of Land Invasions". In: *The Review of Economics and Statistics* 92.3, pp. 505–523. URL: <https://EconPapers.repec.org/RePEc:tpr:restat:v:92:y:2010:i:3:p:505-523>.
- Lujala, PØivi (2005). "The Spoils of Nature – Oil, Gemstones, and Civil Conflict". In: *13th National Conference in Political Science*. Hurdalsjøen.
- Muchlinski, David, David Siroky, Jingrui He, and Matthew Kocher (2016). "Comparing Random Forest with Logistic Regression for Predicting Class-Imbalanced Civil War Onset Data". In: *Political Analysis* 24.1, pp. 87–103. DOI: 10.1093/pan/mpv024.
- Pedregosa, F., G. Varoquaux, A. Gramfort, V. Michel, B. Thirion, O. Grisel, M. Blondel, P. Prettenhofer, R. Weiss, V. Dubourg, J. Vanderplas, A. Passos, D. Cournapeau, M. Brucher, M. Perrot, and E. Duchesnay (2011). "Scikit-learn: Machine Learning in Python". In: *Journal of Machine Learning Research* 12, pp. 2825–2830.
- Petterson, Therése and Kristine Eck (2018). "Organized violence, 1989–2017". In: *Journal of Peace Research* 55.4, pp. 535–547. DOI: 10.1177/0022343318784101. URL: <https://doi.org/10.1177/0022343318784101>.

- Raleigh, Clionadh and Håvard Hegre (2009). "Population, Size, and Civil War. A Geographically Disaggregated Analysis". In: *Political Geography* 28.4, pp. 224–238.
- Russell, Stuart J and Peter Norvig (2016). *Artificial intelligence: a modern approach*. London: Pearson Education Limited,
- Strobl, Carolin, Anne-Laure Boulesteix, Thomas Kneib, Thomas Augustin, and Achim Zeileis (2008). "Conditional variable importance for random forests". In: *BMC Bioinformatics* 9.1, p. 307. DOI: 10.1186/1471-2105-9-307. URL: <https://doi.org/10.1186/1471-2105-9-307>.
- Strobl, Carolin, Anne-Laure Boulesteix, Achim Zeileis, and Torsten Hothorn (2007). "Bias in random forest variable importance measures: Illustrations, sources and a solution". In: *BMC Bioinformatics* 8.1, p. 25. DOI: 10.1186/1471-2105-8-25. URL: <https://doi.org/10.1186/1471-2105-8-25>.
- Tollefsen, Andreas Forø, Håvard Strand, and Halvard Buhaug (2012). "PRIO-GRID: A unified spatial data structure". In: *Journal of Peace Research* 49.2, pp. 363–374. DOI: 10.1177/0022343311431287.
- Vicente-Serrano, Sergio M., Santiago Beguería, and Juan I. López-Moreno (2010). "A Multiscalar Drought Index Sensitive to Global Warming: The Standardized Precipitation Evapotranspiration Index". In: *Journal of Climate* 23.7, pp. 1696–1718. DOI: 10.1175/2009JCLI2909.1. URL: <https://doi.org/10.1175/2009JCLI2909.1>.
- von Uexkull, Nina, Mihai Croicu, Hanne Fjelde, and Halvard Buhaug (2016). "Civil conflict sensitivity to growing-season drought". In: *Proceedings of the National Academy of Sciences* 113.44, pp. 12391–12396.

FUNDING

ViEWS is funded by the European Research Council, grant number 694640 and Uppsala University.



COLLABORATIONS

ViEWS has an active interaction with other projects, including CLIMSEC, CAVE and CROP at PRIO (<https://prio.org/>), the MISTRA Geopolitics project, and most importantly the Uppsala Conflict Data Program (<https://ucdp.uu.se/>) at Uppsala University.

CODEBASE & PUBLICATIONS

ViEWS' codebase is available at:


[https://github.com/
UppsalaConflictDataProgram/
OpenViEWS2](https://github.com/UppsalaConflictDataProgram/OpenViEWS2)

The full pool of publications are accessible at:


[https://pcr.uu.se/research/
views/publications/](https://pcr.uu.se/research/views/publications/)